JIMMA UNIVERSITY

JIMMA INSTITUTE OF TECHNOLOGY

SCHOOL OF CHEMICAL ENGINEERING

POSTGRADUATE PROGRAM IN PROCESS ENGINEERING

MSc. Thesis

Preparation, Characterization, and Application of Lanthanum Doped Magnetic Biochar Composite Adsorbent for Removal of Fluoride from Water

By

Merid Debebe

A thesis submitted to Jimma University, Jimma Institute of Technology, School of Chemical Engineering in Partial Fulfillment of the Requirements for the Degree of Master of Science in Process Engineering

October 2019
Jimma, Ethiopia

DECLARATION

I, Merid Debebe, hereby declare that the thesis, entitled *"**Preparation, Characterization, and Application of Lanthanum Doped Magnetic Biochar Composite Adsorbent for Removal of Fluoride from Water**"* is my own work in agreement with internationally accepted practices; I dually acknowledged and referred all materials used in this work. This work has not been submitted for any academic degree award at any University.

Merid Debebe	_____	_____
Candidate	Signature	Date

This thesis has been submitted with my approval as a university supervisor.

Dr. Job Kasule (PhD)	_____	_____
Main advisor	Signature	Date

This thesis has been submitted with my approval as a university co-advisor.

Mr. Abraha Gebremeskel (MSc)	_____	_____
Co- advisor	Signature	Date

ABSTRACT

Fluoride level more than 1.5mg/L in drinking water is an environmental problem around the world that causes serious health damage for a human. Adsorption is considered one of the best methods for water defluoridation applications. Poor adsorption capacities, long contact time, extremely low or high pH, and high dosage are the major limitations of various adsorbent materials. In the present study, the biochar-based magnetic nanocomposite adsorbent was prepared and applied as an adsorbent for water defluoridation application. The biochar was prepared from waste coffee husk through slow pyrolysis. The composite was prepared by coating iron and lanthanum oxide nanoparticles on the surface of biochar through a chemical co-precipitation method. The magnetic biochar nanocomposite material was characterized by X-ray diffraction analysis (XRD), Fourier transform infrared spectrometry (FTIR), Brunauer-Emmett-Teller (BET), and the surface charge of the adsorbents were evaluated by determining values of pH_{PZC}. The laboratory experiments were carried out using the Central Composite Design (CCD) with four input variables of dosage (2-5 g L^{-1}), solution pH (4–8), contact time (30–70 min), and initial concentration (10–20 mg/L). The optimum conditions for fluoride removal of 98.994 % from water were predicted by the quadratic model (adsorbent dosage of 5g L^{-1}, pH 5.74, contact time 60 min, and initial concentration of 12.245 mg/L) was achieved. The mean triplicate value at optimum conditions resulted in a removal efficiency of 98.51%, which indicates the prediction capability of the proposed response surface model. The results of the present study displayed that the prepared magnetic biochar nanocomposite is a good adsorbent of fluoride.

Keywords: Biochar, Magnetic Biochar, Defluoridation, and Optimization

ACKNOWLEDGMENT

Firstly, I would like to express my thanks to my advisor Dr. Job Samuel Kasule for his support and great advice to complete this paper. In addition, I would like to extend my great thanks to the Process Engineering Chair, Mr. Samuel Gessese for his nice support and delivering relevant information. Next, I would like to say thanks to Jimma University, especially to Jimma Institute of technology for giving me this chance for MSc program. I am also grateful to Addis Ababa University, Department of Chemistry, especially to Ms. Adanech Adera and Dr. Getachew for helping me in the analysis of samples.

Finally, I would like to thanks all my family for their motivation and support all the way through my study period.

TABLE OF CONTENTES

LIST OF TABLES

LIST OF FIGURES

ACRONYMS, ABBREVIATIONS, AND SYMBOLS

WHO	World Health Organization
UNESCO	United Nations Educational, Scientific, and Cultural Organization
IQ	Intelligence Quotient
SNNPR	Southern Nations and Nationalities Peoples of Region
AA	Activated Alumina
UNICEF	United Nations International Children's Emergency Fund
BC	Biochar
LDMBC	Lanthanum Doped Magnetic Biochar
ECRV	Ethiopian Central Rift Valley
FTIR	Fourier Transformed Infrared Spectroscopy
XRD	X-Ray Diffractometer
BET	Brauenner-Emitter-Teller
RSM	Response Surface Methodology
CCD	Central Composite Design
PZC	Zero Point Charge
SEM	Scanning Electron Microscope
FWHM	Full Width at Half Maximum
TISAB	The Ion Strength Adjustment Buffer
CV	Coefficient of Variation
R^2	Correlation coefficient
SD	Standard Deviation

CHAPTER ONE

1. INTRODUCTION

1.1 Background

Fluoride is one of the major water contaminants widely dispersed either naturally in groundwater associated with sediments of volcanic rocks or by industrial effluents (Malago, Makoba, and Muzuka, 2017). Fluoride may be essential for humans and animals' inadequate level for the dental purpose, In contrast, a high level of fluoride consumption can have more serious health problems, it can cause dental and skeletal fluorosis disease (Rouzbahani *et al.*, 2017). World Health Organization (WHO) recommends that the standard fluoride level in drinking water should be below1.5mg/L (WHO report, 2018).

The incidence of high fluoride contamination of groundwater and related health hazards is a worldwide problem (Makoba, and Muzuka, 2017). The geographical area of high fluoride levels in groundwater covers above 28 countries throughout the world that are endemic to fluorosis. From those countries, China, India, Ethiopia, Kenya, and Tanzania are among the most affected countries that have fluoride related serious health problems (Dahi, 2016).

Water defluoridation is the only option to solve the problem of fluoride in drinking water. Currently, wide ranges of fluoride removal processes are being developed such as adsorption and ion exchange, precipitation, coagulation, and membrane separation processes (Singh, 2016). Adsorption is one of the most preferred and widely used methods due to its low cost, high productivity for fluoride removal and its applicability. However, fluoride treatment by adsorption depends upon the adsorbent behaviors i.e. its adsorption capacity; contact time, adsorbent dosage, pH and prevailing water quality after treatment (Mobeen and Kumar, 2017). The most common fluoride treatment by adsorption includes adsorption on activated alumina, ion exchange resin, and bone charcoal. However, they have a better preference for fluoride adsorption, these materials have some limitations regarding efficiency, cost, keeping water quality, and generation of toxic sludge after treatment (Mobeen and Kumar, 2017).

Recent advances in nanotechnology have opened the ways for effective treatment of contaminated water. As many researchers have reported, magnetic metal oxide nanoparticles have higher removal capacity over conventional adsorption materials like activated alumina and bone charcoal. However, they could be expensive due to the use of rear earth metals. Moreover, those metal nanoparticles need to have a supporting material to reduce the suspensions of nanoparticles in the treated water (Bhattacharya, 2017).

The magnetic nanoparticles have an advantage in surface modification of carbonaceous materials for aiming particular contaminant adsorption as well as magnetic separation, which makes the whole process easy (Science and Chen, 2017). Biochar has variable hydrophilic and hydrophobic functional groups. Reports have shown that the surface property of biochar and other carbon materials like graphene oxide and carbon nanotube can be enhanced by impregnating different targeting nanoparticles onto the surface of the material (Tan *et al.*, 2016). According to literature, the Lanthanum element shows comparatively highest electrostatic attraction with fluoride ion than other elements like zirconium, Cerium, and aluminum (Singh, 2016). Researchers have been tried to modify different conventional adsorbents with high valence metal such as irons (III), Lanthanum (III), Cerium (IV), and Zirconium (IV) (Singh, 2016). This is to enhance the fluoride affinity and its adsorption capacity.

In this research work, lanthanum doped magnetic biochar composite adsorbent was synthesized to optimize fluoride adsorption efficiency from contaminated water using response surface methodology. The effects of the adsorption parameters such as adsorbent dosage, solution pH, contact time, and initial fluoride concentration were determined by applying a central composite experimental design. This study was the first report on optimizing fluoride adsorption onto lanthanum doped magnetic biochar nanocomposite adsorbent by response surface modeling.

1.2 Problem Statement

The excessive fluoride in groundwater is a serious global water quality problem. According to UNESCO, more than 200 million people globally use highly fluoride-contaminated water for drinking and cooking purposes. This long-term consumption of high fluoride-containing water can cause dental and skeletal disorders. Additionally, the consumption of concentrated fluoride can cause to reduce brain development and Intelligence Quotient (IQ) scores in children. It can also affect children's cognitive capability hence making them dependent on life and has serious economic and social consequences. Since groundwater serves the main sources of drinking water in the Ethiopian Rift valley area, both dental and skeletal fluorosis disease is a very common public health problem. To solve this problem, Ethiopia still needs financial and technical support from different governmental and non-governmental organizations. In Ethiopian, most of the fluoride treatment plants are not functional at present, which is attributed to the higher cost that incurs to import the media and due to the inherent problems on the available treatment systems. Particularly, adsorption by bone charcoal imparts bad taste, color, and smell; this may not visually acceptable besides its cultural and religious oppositions. Therefore, to solve this challenging problem, there is research need to develop an alternative effective and sustainable technology that takes into account local conditions. The use of lanthanum modified magnetic biochar provides a potential method of an ionic removal through adsorption. Therefore, there is a need to study the removal of fluoride by lanthanum doped magnetic biochar nanocomposite adsorbent.

1.3 Research Objectives

1.3.1 Main objective

The overall objective of the study was preparation, characterizations, and applications of lanthanum doped magnetic biochar composite adsorbent for removal of fluoride from synthetic and natural ground water.

1.3.2 Specific objectives

- To synthesize lanthanum doped magnetic biochar composite adsorbent using coffee husk biochar and metal salts through the chemical co-precipitation method.
- To investigate the physical structure and chemical properties of magnetic biochar nanocomposite material with a focus on its mineralogy, surface chemistry, and porosity.
- To investigate the effect of adsorbent dose, contact time, pH, and initial concentration on fluoride removal efficiency of the synthesized composite adsorbent from synthetic and groundwater samples.

1.4 Scope of the Study

In this study, coffee husk was used as a row material to synthesize biochar and further, it was used for the preparation of lanthanum doped magnetic biochar composite adsorbent. After characterization of the composite material, it was employed as an adsorbent for fluoride removal from water. Batch adsorption study was examined to determine the effects of adsorbent dosage, PH, concentration and contact time on fluoride adsorption efficiency. The quadratic regression model was also developed using response surface methodology to find out the optimum operating conditions of fluoride adsorption process using the composite adsorbent. Fluoride adsorption efficiency of the prepared material on real groundwater also studied. Finally, recyclability and stability of the adsorbent were examined at optimum adsorption conditions, which were predicted by the quadratic model.

1.5 Significance of the Study

This study will provide acceptable information in the development of low-cost and efficient fluoride removal from polluted water. The study is not only relevant to the local context of Ethiopia, but it is a global issue affecting millions of people around the world. Therefore, the result of this study will benefit those people living in rural communities of Ethiopia and other fluorosis endemic countries, which have high fluoride concentration in their groundwater source. The study also will provide economical, sustainable, and locally available solutions to replace other expensive and laborious treatment technologies. Additionally, the method will open a chance for other researchers in acquiring information on the preparation of biochar based magnetic composite materials through chemical co-precipitation methods for different applications.

CHAPTER TWO

2. LITERATURE REVIEW

2.1 Fluoride in Water

There are a number of sources for drinking water in the world; among those, groundwater serves the mainstream especially for areas, which have a shortage of surface water. Unfortunately, water from wells may be contaminated mostly by fluoride, which is a chemical compound that contains a very toxic and highly reactive element of fluorine (F). Both surface water and groundwater may have high fluoride concentration, but the level is often greater in groundwater. Fluoride may be originating from human activities, industrial effluent, and natural process through volcanic activities. The natural existence of fluoride is often associated with weathering of rocks, volcanoes, and geothermal activities (Rajeswari, Kalpana, and Sailaja, 2016).

2.2 Health Effects of Fluoride

Fluoride found in the body is deposited in the bones of human beings and animals. It is a very essential natural element from the point of animal physiology, as a smaller amount up to 1.0 mg/l is important for preventing dental caries and stabilizing the bone structure. However, the conception of the high level of fluoride can cause toxic effects for dental and skeletal problems including crippling fluorosis. According to UNESCO, more than 200 million people globally use highly fluoride-contaminated water for drinking and cooking purposes(Woldemarian, Daniel, and Ershad Khan, 2017; Melaku, 2015)

Source;(Mtalo *et al.*, 2015)

Figure 2.1: Health impacts of fluoride consumption

Table 2.1: Health influences of high fluoride in drinking water

Concentration	Health impacts	Characteristics
1.5-4 mg/L	Dental fluorosis	Mottled enamel or progressive change of teeth From white to brown to black stains.
4-10 mg/L	Skeletal fluorosis	There is stiffness of the backbone and forward bending of the spine is developed and causes for difficulty in walking
>10 mg/L	Crippling fluorosis	Crippling fluorosis is the health effect characterized with a bone junction growing together and difficult for movement
>10 mg/L	Other health impacts	Reduce brain development and Intelligence Quotient (IQ) scores in children, growth retardation, skin irritation, and kidney damage

Source: (Shah and Foundation, 2016)

2.3 Fluoride Standard in Drinking Water

Considering health effects, the WHO guideline recommends the fluoride concentration in drinking water should be falling in the range of 1.0mg/L to1.5 mg/L (WHO report, 2018).

2.4 Global and Ethiopian Scenario

2.4.1 International status of fluoride in groundwater

According to the WHO 2006 report, high fluoride-containing groundwater exists in more than 28 countries globally. This geographical area is mainly covering the Rift Valley belt of Syria and Jordan to Egypt, Sudan, Somali, Ethiopia, Kenya, and Tanzania. The other geographical belt covers the area of Turkey, Iran, India, Afghanistan, Thailand, and China (Dahi, 2016).

2.4.2 Fluoride in Ethiopia

The East African Rift Valley, which spread out from Syria to Malawi and Mozambique that passes through Ethiopia is quite an active volcanic region. Due to the geographical and climatic features, the Ethiopian Central Rift Valley (ECRV) is one of the world's peak fluoride concentrations in the groundwater (Rango *et al.*, 2014). The ECRV region that is facing a high fluoride level in groundwater covers parts of Oromia, Afar, and Southern Nations and Nationalities Regional States (SNNPR). However, the distribution of fluoride in the groundwater is variable, over 40% of shallow and deep wells are polluted with a high level of fluoride in the range of 1.5mg/L to 36mg/L (Teklehaimanot and Mekonnen, 2006).

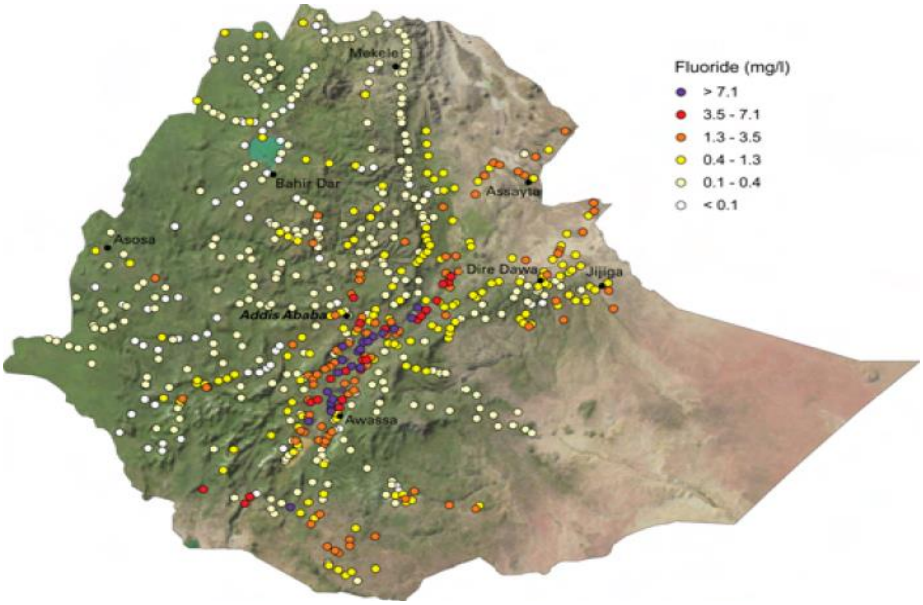

Figure 2.2 fluoride distributions in Ethiopia; (Macdonald and Dochartaigh, 2009)

2.5 Existing Water Defluoridation Technologies

Defluoridation is the process of removing excess fluoride from water and wastewater. Since the time of the knowledge of the hazardous effect of excess fluoride on the health of human beings, numerous methods have been suggested and employing various materials for the removal of fluoride from water/wastewater. The common water and wastewater defluoridation methods that have been used currently can be included in; chemical precipitation, membrane processes and the adsorption process (Mobeen and Kumar, 2017).

2.5.1 Chemical Precipitation

Precipitation methods involve by addition of solvable chemicals to make fluoride precipitates. In this method, various chemicals like lime, magnesium, and aluminum salts have been used as the precipitating agent. Chemical precipitation using lime, alum, and bleaching powder has been widely studied and named as the Nalgonda method. Nalgonda technique is preferred because of the very low cost and due to the eases of handling. However, it needs a daily addition of chemicals in batches and it generates a large amount of toxic sludge every day (Khichar and Kumbhat, 2015).

2.5.2 Membrane Processes

In the membrane defluoridation system, methods using reverse osmosis (RO), electrolysis, and electro-dialysis are effective for removing fluoride salts from water. RO is a very common water desalination technology due to its high efficiency, the ability to remove a variety of contaminants and related with no chemical addition is required. The drawbacks of RO include the high capital cost in running and maintaining the process, there could be a problem of clogging and fouling, and some of the membranes involved in this process (Mobeen and Kumar, 2017).

2.5.3 Adsorption/Ion Exchange

The adsorption process is a physical or chemical phenomenon in which ions or molecules are adhering on the surface of adsorbent due to ion exchange or electrostatic attraction with the solid media. Adsorption is considered the simplest and most cost-effective technique. Water defluoridation using different adsorbents are currently of great interest. The most common fluoride adsorption materials are activated alumina and bone charcoal (Salifu, 2017).

2.6 Criteria to Select Suitable Defluoridation Technology

In developing countries, the challenge encountered for fluoride removal technologies commonly regarding the cost of the power supply, use of chemicals, acceptability of the technology by the society, and regeneration system can be a limit to the application and sustainability of different treatment systems. Therefore, Suitable defluoridation technology should be select mainly by considering its removal efficiency, cost, availability of materials and acceptability of the technology (Waghmare and Arfin, 2015; Khichar and Kumbhat, 2015).

Table 2.2 Comparisons on common water defluoridation technologies

Technology	Advantage	Disadvantage
Coagulation or Precipitation	High efficiency; commercially available chemical	Resulting in toxic sludge, Al residual may present, need PH adjustment need daily addition of chemicals
Membrane filtration	High efficiency; remove other contaminates	High capital high running and maintenance costs toxic wastewater produced
Adsorptive process	Low cost, simple operation, availability of wide adsorbents	High efficiency often demands adjustment and readjustment of pH, some common water ions can interfere fluoride adsorption some material can change water quality

Source; (Shah and Foundation, 2016)

Numerous removal technologies, such as precipitation, ion-exchange/adsorption, Nano filtration, membrane process, and electrocoagulation, have been developed to remove fluoride from drinking water (Abd and Rahman, 2014). Chemical precipitation and adsorption process are the common methods that widely used for water defluoridation. Precipitation is a suitable and inexpensive method, but it needs a high dosage of chemical addition frequently. Furthermore, the addition of chemicals can increase the alkalinity of the water after treatment. Fluoride treatment using precipitation method shows excess residual fluoride in the treated water, which is usually higher than the allowable limit of fluoride in drinking water. Adsorption is considered as highly effective, inexpensive, and sustainable defluoridation methods because of the availability of numerous fluoride selective materials, easy treatment system, and low operating cost (Waghmare and Arfin, 2015).

2.7 Common Fluoride Adsorbents

2.7.1 Activated alumina (AA)

The water defluoridation process using activated alumina (Al_2O_3) is an efficient material in the removal of fluoride from water. Fluoride treatment using activated alumina shows limitations in some cases regarding the requirements of pH adjustment before and after treatment, generation of high fluoride-containing spent generation, which is challenging to dispose of (Patra *et al.*, 2018).

Figure 2.3: Photo of activated alumina (AA)

2.7.2 Bone charcoal

The major constituents of bone char are calcium carbonate, calcium phosphate, and activated carbon. Since fluoride ion is highly selective by calcium and phosphate, bone char is a very encouraging material in the removal of fluoride. However, the preparation method has some influences on removal efficiency and water quality. Poor quality bone charcoal can impart bad taste, color, and smell, this may not visually acceptable, it may offer cultural and religious oppositions (Kanyora *et al.*, 2015).

$$Ca(PO_4)_6.CaCO_3 + 2F^- \rightarrow Ca(PO_4)_6.CaF_2 + CO_3 \qquad \text{(R-1)}$$

Bone charcoal, which prepared by carbonizing above 1000 °C, had greater fluoride removal efficiency compared with that of bone charcoal which produced at lower carbonization temperature (Mobeen and Kumar, 2017).

2.8 Current Status of Water Defluoridation System in Ethiopia

In Ethiopia, fluoride removal technology still needs financial and technical support from different governmental and non-governmental organizations. Currently, Precipitation using aluminum sulfate and adsorption using bone charcoal are the two common and available defluoridation systems. However, most of the treatment systems have become out of service due to the integral limitations of the available treatment systems (Sara Datturi, Assefa Kumsa, Seifu Kebede, 2017). The final concentration of fluoride in the treated water using bone charcoal and aluminum sulfate shows still above level prescribed by the World Health Organization (WHO), this may cause dental fluorosis (Bekele Abaire, 2009).

From practical observations, various limitations on the available fluoride removal techniques were observed in the areas of the central rift valley of Ethiopia. In the specified area, various household and multistage treatment plants have become out of service including larger treatment plants such as Adama Wonji/Shoa and Ziway water supply treatment plants.

Figure 2.4: (A) Ziway water supply treatment plant (not functional at present); (B) Functional fluoride treatment plant using aluminum sulfate (Tejitu village)

According to (N, UKaid, 2002) report, the Ziway water treatment plant was implemented with an initial investment of 29,500,000 Ethiopian Birr to serve about 41,420 people from the total population of 43,610 in Ziway town. The plant was projected to treat Ziway lake water using different agents including aluminum sulfate.

However, it is not functional at present due to the presence of aluminum suspension and excess fluoride in the treated water. The small communities around Ziway Lake still use the lake as a drinking water source, which has high fluoride up to 30 mg/L. The other observation from Tejitu village (near Alem Tena town) indicates that peoples of rural communities of Ethiopia are facing challenges to get fluoride-free water. This can be taken to validate the limitations of the available treatment systems. A similar observation has been reported in different parts of Ethiopia (Sara, Assefa Kumsa, Seifu Kebede, 2017). Therefore, to solve this challenging problem, there is research need to develop an alternative effective and sustainable technology that takes into account local conditions.

2.9 Advanced nanomaterial's for fluoride removal

Recent advances in nanotechnology have opened the ways for effective treatment of contaminated water in place of conventional technics due to its low cost and high efficiency (Abd and Rahman, 2014). This would have an advantage for developing nations like Ethiopia, as an adsorbent for cleaning water pollutants from water/wastewater. Nanostructured materials like magnetic nanoparticle, metal oxides, and carbon-based composites have become a current research focus for the treatments of fluoride ions, charged particles, and other pollutants from water (Samanta, Das, and Bhattachajee, 2016).

2.9.1 Fluoride adsorption using magnetic composite materials

Magnetic filtration is an emerging water treatment technology that can provide rapid and efficient removal contaminants from water and wastewater. The use of magnetic nanoparticles (magnetite Fe_2O_4) has an advantage for surface modification of materials for targeting particular pollutant remediation like fluoride and other contaminants as well as magnetic separation that makes the synthesizing, filtration and regeneration processes easy (Sharma *et al.*, 2018).

From recent studies, it was observed that numerous magnetic composite adsorbents have been synthesized for the treatments of fluoride. The magnetic adsorbents synthesized using cerium and titanium with magnetite ($Ce–Ti@Fe_3O_4$) have higher fluoride adsorption capacity of 91.04 mg/g at conditions of normal pH water, whereas composites of magnetite with zirconium oxide ($Fe_3O_4@ZrO_2$) also shows very high adsorption capacity (158 mg/g) at very low pH condition. The composites of magnetite with Zr(IV)–poly (acrylamide) shows interesting fluoride

adsorption capacity of 124 mg/g in normal pH water. The other interesting Nano-adsorbent synthesized from magnetite, silver, and lanthanum (FeO_4@Ag-La) shows higher capacity up to 45.320 mg/g at pH 4; in addition, these composite materials found that other co-anions like Cl^{-}, $SO4^{2-}$, HCO^{3-} and PO_4^{3-} found has almost no effect on fluoride adsorption (Sharma *et al.*, 2018).

However, most of those high efficient fluoride adsorbents could be expensive due to the use of rear earth metals. Moreover, those metal nanoparticles need to have a supporting material to reduce the suspensions of nanoparticles in the treated water. Compositing metal nanoparticle with carbon-based material has an advantage regarding economic perspective as well as its stability (Abd and Rahman, 2014). Thus, there is a need to develop cheap and sustainable water defluoridation technology.

2.9.2 Water defluoridation using biochar based composite material

Water refining using biochar based material is comparatively a new practice. Biochar is a type of carbonaceous materials, which can be prepared from different biomasses through the thermochemical conversion in an oxygen-free environment. The surface of biochar has variable hydrophilic and hydrophobic functional groups. Typically, its surface is dominated by negatively charged heterogeneous compositions with higher pH value. This makes the biochar excellent for metal cation removal due to specific adsorption on oxygen-containing functional groups, but it is poor for anionic pollutants (Akbarnezhad and Safa, 2018).

Biochar based nanocomposite is receiving attention for the researcher because of their higher surface area, porosity, and good ion exchange capabilities. Biochar can be modified by impregnating different metal oxides, clays, and other targeting elements on its surface. In this argument, the biochar is fundamentally used to support the materials being deposited on the surface. Thus, the impregnation of metal oxide nanoparticles on the surface of biochar leads to an increase of adsorption capacities of different anionic water pollutants like phosphate, fluoride, chloride, and nitrates (Akbarnezhad and Safa, 2018).

Table 2.3: Fluoride adsorption capacities of different biochar based composites

Biochar based composites	Adsorption Conditions	Adsorption		Reference
		Capacity (mg/L	Efficiency (%)	
Iron modified Biochar	At pH 6, Dose 10 g/L, at room temperature	3.928	90	(Xuebin *et al.*, 2018)
Magnetic biochar	At pH 2, equilibrium time (50 min), and dose (0.75 g/L)	4.99	90	(Mohan, Kumar and Srivastava, 2014)
Modified tea waste biochar	At pH 2, at 25 ^{o}C	52.47	98.2	(Roy, 2017)
Lanthanum doped Nano magnetite graphite carbon	At natural PH, Room temperature	77.12	__	(Wen, Wang, and Dong 2015)
Lanthanum modified biochar	pH 6, contact time 50 min, dose 5 g/L, 25 ^{o}C	164.23	99.6	(Habibi, Rouhi and Ramavandi, 2018)

By considering the benefits of magnetic filtration in the synthesizing and regeneration process, inexpensive magnetic biochar composite adsorbents could be developed for fluoride removal. Also, researchers have proved that lanthanum (La) doped adsorbents can increase the fluoride removal capacity; this is due to the high affinity of lanthanum with fluoride ion (Habibi, Rouhi and Ramavandi, 2018). Therefore, considering the above interesting ideas, lanthanum doped magnetic biochar (LDMBC) was selected as relatively economical and efficient fluoride adsorbent by considering related studies as a basis.

2.10 Magnetic Biochar Composite Fabrication Methods

Biochar modifications can be conducted using either a pre-treatment system or post-treatment by means of a chemical co-precipitation method (Tan *et al.*, 2016). Generally, metal oxides impregnation onto biochar is achieved by soaking raw biochar or their feedstock into the solutions of metal salt solutions followed by heating under atmospheric conditions. Studies have shown that the heating process in temperatures ranges from 50 to 300 °C is very necessary to drive off nitrates or chlorides in gas form. During the thermal treatment, the metal ions could be oxidized to form metal oxide nanoparticles on the surface of biochar (Domingues *et al.*, 2017).

2.10.1 Chemical co-precipitation method after biochar pyrolysis

A modification of biochar using this method involves the treatment of biochar using metal nanoparticles after the pyrolysis process. The objective of this composite fabrication method is to spread out of targeted nanoparticles over the surface of biochar. The biochar is fundamentally used as a porous carbon platform to support magnetic nanoparticles (Gingasu *et al.*, 2011).

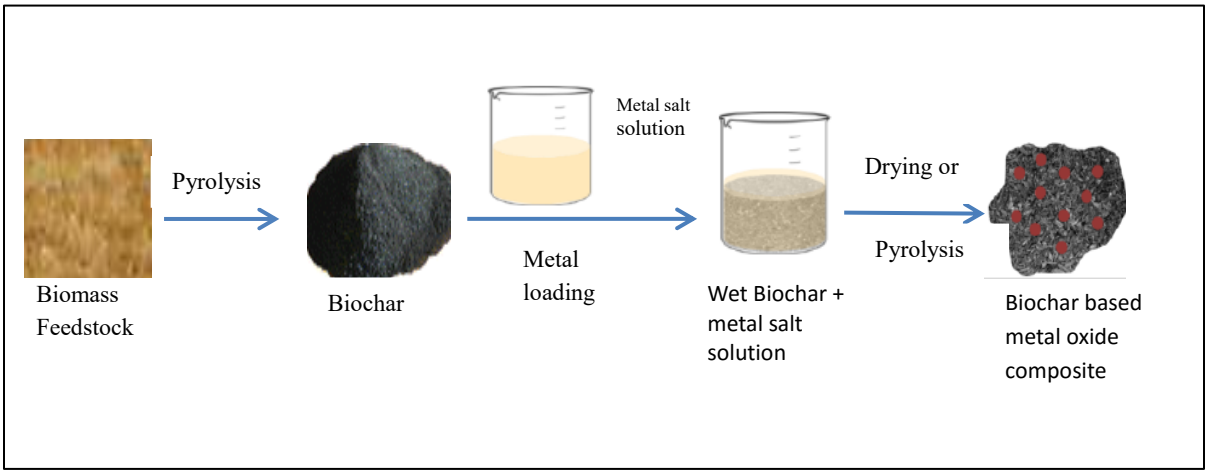

Figure 2.5: Process flow diagram of metal impregnation onto biochar after pyrolysis

Magnetic biochar in the chemical co-precipitation method is mostly conducted by direct precipitation of iron species onto biochar after pyrolysis. The key influencing factor in the magnetization process is the amount of alkali in the solution (Gingasu *et al.*, 2011). In the Gingasu report (Gingasu *et al.*, 2011), two possible reactions were developed for magnetite formation in the alkali solution.

$$NH_4OH \leftrightarrow NH_4^+ + OH^-$$
$$Fe^{2+} + 2Fe^{3+} + 8OH^- \rightarrow Fe_3O_4 + 4H_2O \qquad \text{(R-2)}$$

$$3Fe^{2+} + [NH_3OH]^+ \xrightarrow{+6OH^-} Fe_3O_4 + NH_4^- + 3H_2O \qquad \text{(R-3)}$$

Similarly, researchers use NaOH solution as an alkaline source to develop magnetite (Fe_3O_4) on biochar surface (Mohan, Kumar and Srivastava, 2014).

2.10.2 Chemical co-precipitation before pyrolysis process

Metal oxides impregnation onto biochar is achieved by soaking raw feedstock into the solutions of metal salt solutions followed by heating under atmospheric conditions. In the post pyrolysis process, syngas's, nitrates, chlorides, and other lower molecular weight organics could be driven off as a gas form. Thus the surface of carbon can be modified due to the activities of metal nanoparticles (Domingues *et al.*, 2017). This composite fabrication process is effective to impregnate nanoparticles on carbon surfaces. However, there is a limitation regarding solid-liquid separation after biomass treatment with the metal salt solution (Gingasu *et al.*, 2011).

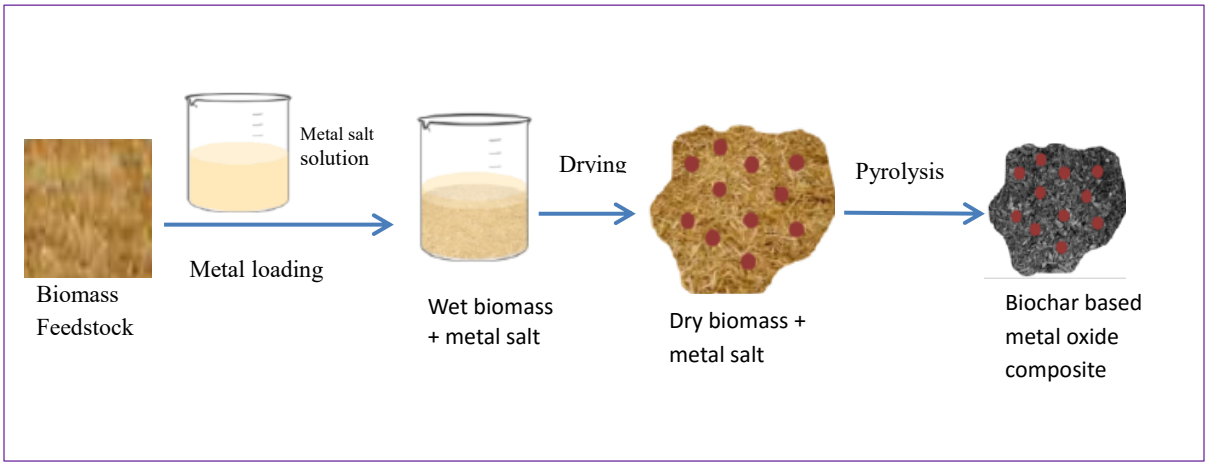

Figure 2.6: Process flow diagram of metal impregnation onto feedstock before pyrolysis

Generally, metal oxides impregnation onto biochar is achieved by soaking raw biochar or their feedstock into the solutions of metal salt solutions followed by drying and pyrolysis (Boshir *et al.*, 2016).

2.11 Surface Chemistry of Biochar and Magnetic Biochar

Typically, biochar family is mainly amorphous with some limited crystalline structures of randomly interconnected aromatic sheets. After doping metal oxide nanoparticles (i.e. ϒ-Fe_3O_4), the different surface functional groups (e.g.,–OH) on the biochar become reduced due to the existence of a surface redox reaction. The surface chemistry of biochar is clearly reported by including chemical structures of row biochar as shown in Figure 2.5 bellow (Cheng and Li, 2018),

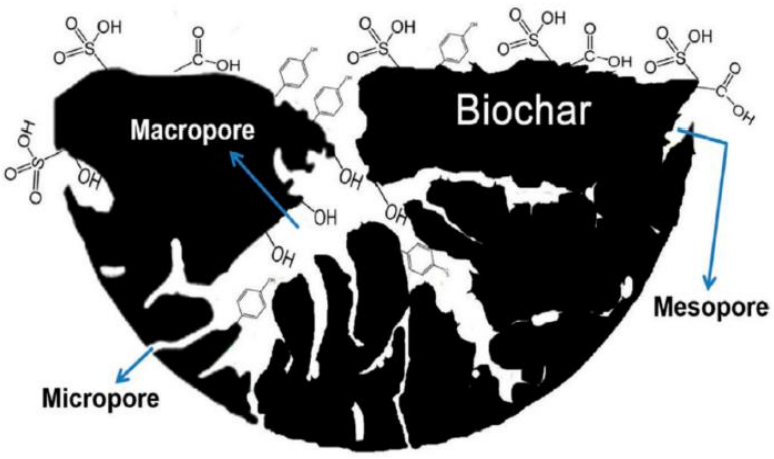

Figure 2.7: Schematic representation of porous biochar with different functional groups

In the literature, two ideas have been reported related to the effects of metal nanoparticle on surface area and porosity of carbon material. If the carbon material has initially lower surface area, then the iron species can act as an activating agent to make micro and mesopore on the carbon surface, this leads to increase the surface area after modification (Cheng and Li, 2018). In other cases, the impregnation of metal nanoparticle onto high surface area material can reduce its surface area after impregnation. This is due to the obstruction of macropore by metal nanoparticle (Kakavandi *et al.*, 2013).

According to Kakavandi report, the surface area of activated biochar (1301 m^2/g) becomes reduced almost by 50% to 671.2 m^2/g after combined with magnetite ($C@Fe_3O_4$) on the carbon surface. Since biochar has initially lower surface area, the surface area of biochar after treating with metal salts gives higher specific surface area and porosity (Cheng and Li, 2018). This increased surface area for a biochar based composite agrees with other studies as described in Table 2.4 as follows;

Table 2.4: Effects of metal nanoparticles on biochar surface area

Feedstock	Adsorbent	synthesizing methods	Surface area (m^2/g)	Reference
Coffee Husk	Biochar	Hydrothermal @ 108 °C for 3.5 h	48.84	(Hien *et al.*, 2017)
	Magnetic biochar	Co-precipitation after carbonization	142.32	
Corn-cob	Biochar	Pyrolysis @650 °C for 3 h	158	(Tu, 2017)
	Magnetic biochar	Co-precipitation after pyrolysis	303.1	
Tamarix hispoda tree	Biochar	Pyrolysis @650 °C for 2 h	---	(Habibi, Rouhi and Ramavandi, 2018)
	La-doped biochar	Co-precipitation method	164.52	

Therefore, it can be concluded that biochar magnetization using iron species can increase the surface area and porosity of biochar.

2.12 Biochar from Coffee Husk

Coffee husk is the major solid residues from the processing of coffee after hulling the coffee beans. The various types of coffee been residues can be changed into biochar. According to the previous studies, the coffee husk moisture content is lower (~14%), this Leads the conversion into biochar much easier than other residues like pulp. The yield obtained after coffee husks pyrolysis at temperatures ranges from 350°C to 550°C varies from 43.5% - 31.6% (Cheng and Li, 2018).

Table 2.5: The proximate analysis of coffee husk biochar

Temperature(^{o}C)	Yield (%)	Fixed carbon	Ash	Volatile matter
350	43.5	52.5	12.9	34.6
450	37.7	60.9	12.9	26.2
550	31.6	62.8	19.6	17.6

Source: (Dume, Berecha and Tulu, 2015).

2.13 Coffee Husk Availability in Ethiopia

In Ethiopia, coffee husk has been generated over the past decade in the parts of Oromia and Southern parts of Ethiopia. The volume of coffee production in Ethiopia is estimated at about 426,000 metric tons in 2018/19 and the coffee husk yield was estimated to be 170,400 metric tons (Francom and Counselor, 2018). From practical observation, the coffee husk is left unused and disposed of by burning in the fields except for food cooking purposes in some towns (i.e. Jimma). Improper disposal contributes to a major environmental problem. Thus, the conception of sustainable development and advanced techniques for the profitable and acceptable use of this type of residue are being required.

Therefore, the coffee husk can be used as a carbon source in the development of sustainable and inexpensive magnetic biochar composite adsorbent, which can be applicable in developing countries like Ethiopia. Since there is only a few studies have been published regarding water defluoridation using biochar based composites material, waste coffee husk was used in this study as a starting material to prepare biochar based magnetic composite adsorbent for water defluoridation application.

2.14 Factors Affecting the Rate of Fluoride Adsorption

The factors affecting fluoride adsorption parameters such as adsorbent dose, contact time, pH, initial concentration, and co-existing anions needs more study to find the optimum conditions that could give higher removal efficiency using biochar based material (Zhang *et al.*, 2017).

2.14.1 Effect of pH

The PH of the solution is an active parameter to affect fluoride adsorption from water; the previous studies explained that the absorption efficiency of fluoride in acidic solution increases due to electrostatic attractions between cationic surfaces and fluoride ion. In contrast, fluoride removal efficiency decreased in basic solution due to the presence of great numbers of hydroxide (OH^-) ions, which may compete with negatively charged fluoride ion. Therefore, the pH of the solution has a major effect on fluoride adsorption (Habibi, Rouhi and Ramavandi, 2018).

2.14.2 Effect of adsorbent dose

The high amount of adsorbent dosage of the material results in increased removal of the contaminants from aqueous solution. This is because attributed to higher accessibility of surface and pore volume at higher adsorbent doses (Zhang *et al.*, 2017).

2.14.3 Effect of initial concentration

The fluoride removal efficiency of the adsorbent gets tired with an increase in the initial concentration of the fluoride in the aqueous solution. This is because the adsorption sites for a fixed amount of adsorbent materials become limited at high concentrations (Ali *et al.*, 2018).

2.14.4 Effect of contact time

Contact time between the aqueous solution and the prepared adsorbent media is a major factor in the defluoridation system. Studies have shown that the rate of fluoride removal from water using magnetic biochar nanocomposite material shows higher at the beginning of the treatment process (Roy *et al.*, 2018).

2.14.5 Effect of interfering ions

Aqueous solutions may contain different anions such as carbonate, chloride, nitrate, phosphate, and bicarbonate in addition to fluoride, these anions can compete with fluoride and cause to reduce the removal efficiency (Nabizadeh and Sadjadi, 2015).

CHAPTER THREE

3. MATERIALS AND METHODS

3.1 Description of the Study Area

The study area of this research work was part of the Ethiopian Central Rift valley (ECRV), which are facing excessive fluoride in their groundwater, the area covers the administrative borders of Oromia, Afar and Southern parts of Ethiopia. The region is found in the Great East African Rift Valley, which extends from Syria to Mozambique. The area is characterized by high volcanic and basaltic rocks, which is the reason to release excessive fluoride into the groundwater.

3.2 Chemicals

All analytical grade reagents used in this study such as ferric chloride hexahydrate ($FeCl_3 \cdot 6H_2O$), ferrous chloride ($FeCl_2.4H_2O$), lanthanum Chloride ($LaCl_3$), hydrochloric acid (HCl), potassium nitrate (KNO_3), sodium hydroxide (NaOH), ethylenediaminetetraacetic acid (EDTA), sodium chloride (NaCl), and sodium fluoride (NaF) were analytical grade and purchased from Rankem industry and trading PLC.

3.3 Apparatus

Tubular paralyzer reactor was used to prepare biochar from the coffee husk. Magnetic stirrer, oven drier, and other types of equipment were used to prepare lanthanum doped biochar-based magnetic composite adsorbent. X-ray diffraction (XRD-7000, USA model) equipment, Fourier transform infrared spectroscopy (FTIR), thermo gravimetric analysis (TGA-400), Brunauer-Emmett-Teller (HORIBA SA9600 USA model), and Scanning Electron Microscope (SEM) equipment were used to investigate the physicochemical analysis of the adsorbent material. Fluoride Eon-Selective electrode (ISE) was used to measure the concentration of fluoride in the aqueous solution.

3.4 Sample Collection

Waste coffee husk was collected from Jimma local coffee hulling enterprises as a starting material in adsorbent preparation. To investigate the effects of co-anions in the fluoride adsorption process, well water samples were collected from the areas of Central Rift valley of Ethiopia, particularly from Ziway town, Meki town, and Alem Tena town. After collecting the samples, the initial fluoride concentration, pH, and other parameters for each ground water sample were analyzed. Finally, the groundwater samples were treated using the prepared composite adsorbent at optimum conditions predicted by the quadratic model.

3.5 Adsorbent Preparation

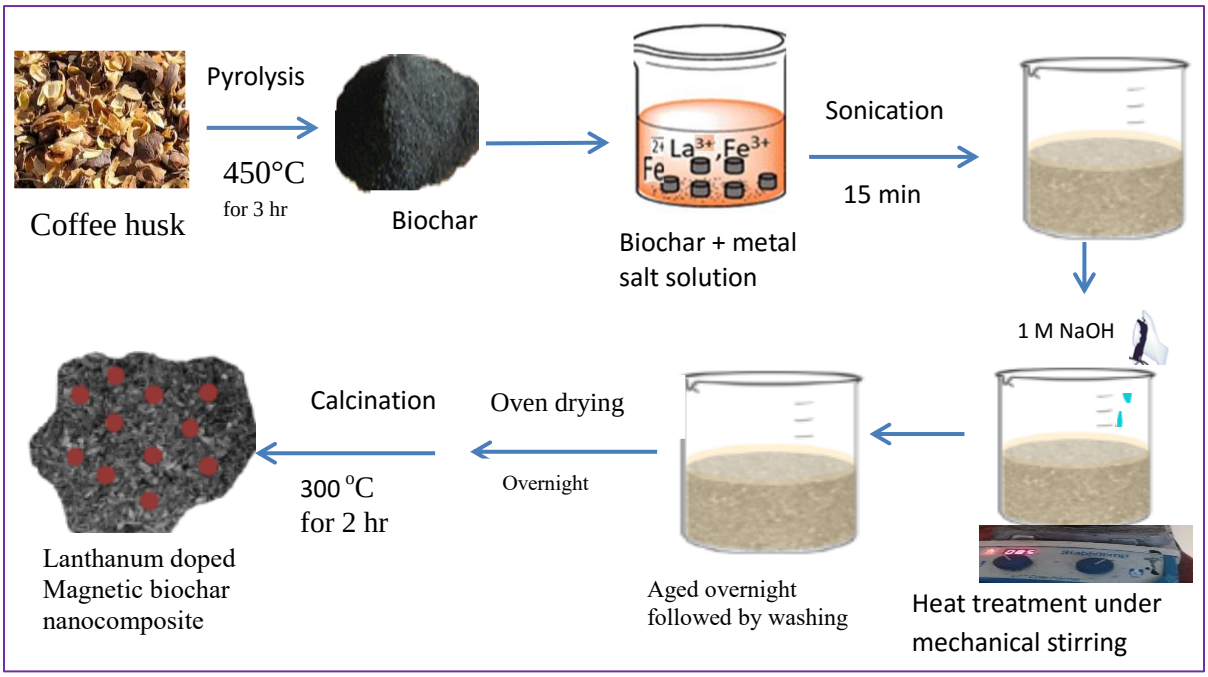

Figure 3.1: Adsorbent preparation graphical flow sheet

3.5.1 Synthesis of Biochar from Coffee Husk

The collected row coffee husk was washed with tap water followed sun-dried for 2 days. Then it was subjected to a tubular pyrolyzer at 450°C for 3hrs in the absence of oxygen. After completing the carbonization process, it was cooled overnight in a pyrolyzer. Finally, the prepared biochar was ground and sieved to obtain the particle size of <75 μm and stored in a glass bottle for further use.

3.5.2 Preparation of lanthanum doped magnetic biochar nanocomposite adsorbent

Biochar based magnetic nanocomposite adsorbent was synthesized by using iron and lanthanum salts as an activating agent through a chemical co-precipitation method. As a pre-test, two experimental trials were conducted. The one without the presence of lanthanum salt and the second with the ratio of $LaCl_3$ to Biochar (0.25w/w) were applied. From the two trials, magnetic biochar with the presence of lanthanum shows higher fluoride removal efficiency and thus, it was selected for further adsorbent preparation by considering recent works with some modifications (Akbarnezhad and Safa, 2018: Tang *et al.*, 2019).

Briefly, biochar powder (10 g) was dispersed into a flask containing 100 mL of deionized water, and sonication for colloidal dispersion. The dispersion was mixed with 100 ml of an aqueous solution containing $FeCl_2$ (3.17 g), $FeCl_3$ (8.11 g) and $LaCl_3$ (2.453 g) followed by sonication again for 15 min. After sonication, the NaOH (1M) solution was added into the solution until the pH of the solution reached 10 -11 at room temperature. To complete the reaction, the whole mixture was stirred at 85 ^oC for 24 hrs, and it was cooled to room temperature. Then, the black precipitate was separated through a 42-μm whatman filter with the help of an external magnet and washed repeatedly with deionized water until the pH decreased to seven. Then, the final precipitate was dried in an oven overnight followed by calcination in a muffle furnace at 300 ^oC for about two hrs. Finally, the milled lanthanum doped magnetic biochar (LDMBC) composite adsorbent was passed through the 1 mm sieve to obtain the constant particle size.

3.6 Characterization of Materials

3.6.1 Proximate analysis

As per ASTM standards, the proximate analysis of coffee husk was analyzed using the following standard methods.

3.6.1.1 Moisture content

The size-reduced coffee husk sample was left in an oven (105 ^{o}C) for a period of 24 hours to being dried. The mass of the sample was measured every 6 hours interval until a constant mass is obtained. The initial weight and the final weight were used to calculate the moisture content.

$$Moisture\ (\%) = \frac{(w_1 - w_2)}{w_1} * 100\ \% \qquad (3.1)$$

Where w_1 = weight of coffee husk before drying (g)

w_2 = weight after drying (g)

3.6.1 2 Volatile matter

The volatile content of organic compound was examined after ignition the dry sample in a furnace (450 ^{o}C) for 30 minutes. The sample was sent to a desiccator for about 20 minutes and weighed.

$$\text{Volatile Mater}\ (\%) = \frac{(w_1 - w_2)}{w_1} * 100\ \% \qquad (3.2)$$

Where w_1 initial weight before burning (g)

w_2 weight after burning (g)

3.6.1.3 Ash Content

The oven-dried sample was weighed and put in an open crucible in a furnace at 450 °C for 2 hours. The final remaining matter after ignition is the ash content and calculated as follows.

$$\text{Ash content}\ (\%) = \frac{w_1}{w_2} * 100\ \% \qquad (3.3)$$

Where w_1 weight of ash (g)

w_2 weghit of sample after oven dried (g)

3.6.1.4 Fixed Carbon

Fixed carbon was calculated by subtracting the sum of the percent moisture, ash, and volatile matter from the total content of the sample. Thus, the fixed carbon was calculated as

$$FC = 100 - (moisture\ content + ash\ content + volatile\ matter) \quad (3.4)$$

Where FC fixed carbon (%)

3.6.2 Yield of biochar

The percentage yields of coffee husk derived biochar at 450 ^{o}C were evaluated using laboratory furnace for pyrolysis time of 2 hrs (limited oxygen) and tubular pyrolyzer (oxygen free) for 3 hr. The yields of the two analyses were calculated using the following equation

$$yield\ (\%) = \frac{Weight\ of\ biochar\ produced}{weight\ of\ pyrolized\ feedstock} \quad (3.5)$$

3.6.3 Bulk density of materials

The dry empty and cleaned 14 ml centrifuge tube was weighed as w_1. The same tube was filled with the sample and weighed again as w_2. The bulk density was calculated by dividing the weights the sample to the volume of centrifuge tube as follows.

$$\text{Bulk Density} = \frac{(w_2 - w_1)}{\text{Volume of centrifuge tube}} \quad (3.6)$$

3.6.4 Point of zero charge examination

Typically, a particular material has a characteristic pH at which it is neutral. The pH value at which the surface is neutral is called the point of zero charges (PZC). The point of zero charges (PZC) for Biochar and LDMBC was investigated by the solid addition method (Rechcigl *et al.*, 2015). 500ml of KNO_3 (0.1M) in the pH range of 3 to 10 was prepared in 8 different flasks. 45ml of KNO_3 (0.1M) was taken from the 500ml, the initial pH of the solution was adjusted by adding drops of 0.1N NaOH, and 0.1N HCl solutions and 0.5 g of powdered Biochar (BC) and LDMBC samples were added in each flask and shaken at room temperature. After 48 hrs, the final pH of all samples was measured and plotted against ΔpH. The intersection point of the curve with the line passing through the origin is taken as a reference for deciding the point of zero charge value.

3.6.5 Fourier transform infrared spectroscopy analysis (FTIR)

The infrared spectra of the prepared materials were recorded using FTIR in transmittance mode. FTIR analyzer was used for the analysis of the bond stretching and vibrations of functional groups. It was carried out at room temperature using Spectrum 400-IR (Perkin Elmer) in the range 4000-400 cm^{-1} using KBr pellets as a reference. Then chemical functional groups were determined by examining wavenumber associated with signals according to standard absorbance of functional groups in the FTIR spectra.

3.6.6 Thermogravimetric analysis

Thermal stability of both BC and LDMBC was examined using a thermogravimetric analysis (TGA) analyzer to measures the amount of weight loss of the sample as a function of increasing temperature, or isothermally as a function of time in a nitrogen atmosphere.

3.6.7 X-ray diffraction analysis

X-ray diffraction (XRD) analyses of the prepared materials powder were examined using the instrument (XRD-7000) at Jimma University, Laboratory of Material Sciences Engineering. The analyses were conducted at an accelerating voltage of 40 kV and the radiation current 30 mA within the choice of diffraction angle 2θ =10-80^{o}.

Determination of average crystalline size

Crystalline size and average crystalline size of biochar based magnetic nanocomposite adsorbent were determined from XRD data using Scherrer's question.

$$D = \frac{k\lambda}{\beta \cos\theta} \qquad (3.7)$$

Where: - D=crystallite size (nm)

k=0.9 (Scherrer's constant)

λ=0.15406 (wavelength of the x-ray sources)

β=Full Width at Half Maximum (FWHM)

θ=peak position (radians)

First peak position and FWHM were determined from XRD data, then the average crystalline size was determined by using Microsoft excel.

3.6.8 Scanning electron microscopy analysis (SEM)

The SEM analysis of the BC and LDMBC samples were conducted in Addis Ababa Science and Technology University. This analysis was performed to examine the changes in surface morphology of the biochar before and after modification using iron and lanthanum oxide nanoparticles.

3.6.9 Surface area

The specific surface area of coffee husk biochar, magnetic biochar, and lanthanum doped magnetic biochar were determined by nitrogen adsorption using the HORIBA instrument (HORIBA SA9600 USA model). The Brunauer-Emmett-Teller or BET method was used by determining the volume of adsorbed nitrogen gas based on adsorption and desorption of different gas concentration at atmospheric pressure and room temperature. The three samples were initially treated at 230 ^{o}C for 1 hr. in order to remove air and water molecules from the pore. Finally, the samples were analyzed as shown in Figure B-6.

3.7 Solution Preparation

2.7.1 Preparation of stock and standard fluoride solutions

A stock of fluoride solution with having a concentration of 1000 mg/L was prepared by dissolving a measured 2.21 g of sodium fluoride (NaF) in 1 L of distilled water. Then the standards of the working solution were prepared from the stock solution by series dilution method using distilled water as required (i.e. 100, 10, 1, 0.1, 0.01) for the calibration of the ion-selective fluoride electrode (i.e. detection limit 0.02) to be used for sample reading. In addition, the solutions of different initial concentrations were prepared as required from the stock solution.

3.7.2 The ion strength adjustment buffer solution

The ion strength adjustment buffer (TISAB) solution was prepared according to standard procedures as follows (Thermo Scientific Orion, 2011). In a volumetric flask containing 500 ml of deionized water, 57 ml of glacial acetic acid, 58 g of NaCl, 7 g of sodium citrate and 2 g of EDTA were added and allowed to dissolve. Then the pH of the buffer solution was adjusted to be 5.3± 0.2 with 0.1M sodium hydroxide and then made up to 1 L in a volumetric flask with deionized water.

3.8 Batch Adsorption Experiment

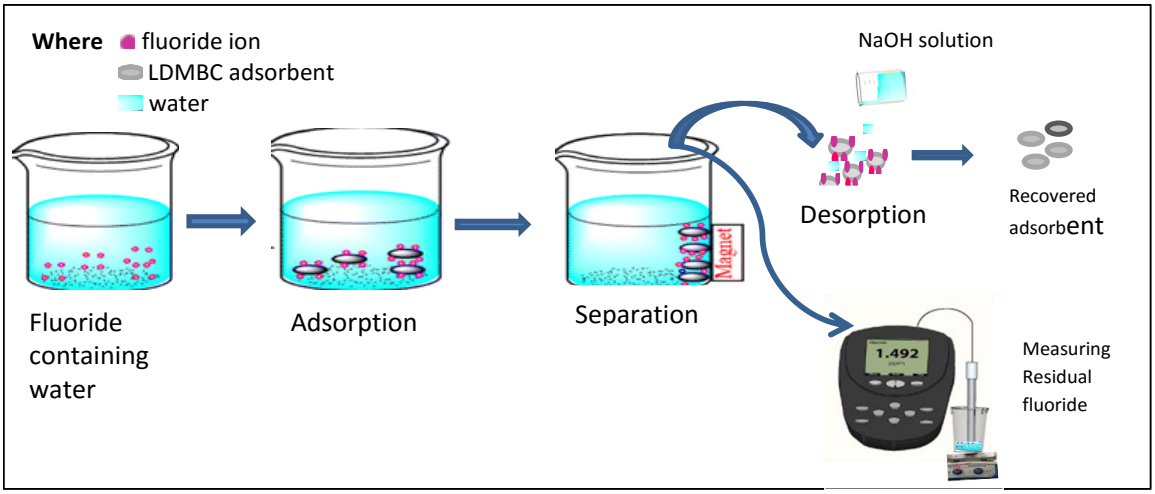

Figure 3.2: Adsorption experiment graphical flow sheet

Batch adsorption studies were conducted in 250-mL glass beakers with 100 mL of fluoride working solutions with a designed concentration and pH values. All the pH of the solutions was adjusted using 0.1N HCl or 0.1M NaOH solution. After adding the required amounts of LDMBC adsorbent, at room temperature, the flasks were stirred isothermally in a magnetic stirrer at 160rpm. Then the samples were taken at a different time according to the RSM design matrix. Then the residual fluoride concentration in the sample solutions was determined using Fluoride Ion-Selective electrode (FISE) in Addis Ababa University at the laboratory of analytical chemistry.

3.9 Electrode Calibration

The instrument was calibrated according to the FISE manual before measuring residual concentration (Thermo Scientific Orion, 2011). The calibration was conducted by using the prepared10 mL of the 100, 10, 1, 0.1, and 0.01 mg/L fluoride solutions together with 10 mL of TISAB II. After getting correct readings in every five points, the results were saved in the instrument and ready to measure fluoride content in water samples.

3.10 Fluoride Measurement Using FISE

After the calibration FISE instrument, it was used to examine the residual fluoride concentration in the filtered water samples. To prevent interference of other ions, water samples were mixed with TISAB solution (1:1) in a small plastic beaker, which contains 10 ml of treated water sample and 10 ml of TISAB solution. Then the solutions were mixed in a magnetic stirrer for about 2–3 min. finally, the residual fluoride content in the treated water samples was obtained directly from the electrode potential in milligram per liter of solution. The percentage of removal of fluoride ions and adsorption capacity were calculated from the following mass balance equations:

$$\mathrm{E}\ (\%) = \frac{(C_0 - C_t)}{C_0} * 100 \qquad (3.8)$$

$$q_t = \frac{(C_0 - C_t)}{m} * V \qquad (3.9)$$

Where E (%) removal efficiency, q_t (mg/g) is the amount of adsorbed at any time t, C_0 (mg/L) is the initial fluoride concentration and C_t (mg/L) is the concentration of fluoride in the sample at any time t. V (L) is the volume of the aqueous solution.

3.11 Experimental Design and statistical analysis

The response surface methodology (RSM) was used to study the adsorption process of fluoride ion from water using magnetic biochar nanocomposite adsorbent. Central composite design (CCD) is a common and efficient design in RSM; it was selected as a designing tool to investigate the interactive effect of process variables and in building mathematical models to describe the overall fluoride adsorption process. To study the process parameters, the four major factors (pH, adsorbent dose, initial concentration, and contact time) were selected as independent parameters, and percent of fluoride removal was taken as the response of the design. Ranges of factors were selected by considering the previous related works. The pH of the solution was designed to vary in a wide range from 2-10, which helps to clearly identify its effect on fluoride adsorption efficiency of the material.

The average fluoride concentration in rift valley of Ethiopia was reported as it is 10 mg/L (Teklehaymanot, and Mekonnen, 2006). Therefore, the initial concentration was designed to be in range between 5 and 25, which consider the lower and higher concentrated groundwater in Ethiopia. By considering the cost of adsorbent material, lower adsorbent dose is recommended in the literature. However, at lower dose below 1g/L shows lower removal efficiency. Since central composite design (CCD) consider –alpha and +alpha value, adsorbent dose between 2 g/l and 5 g//L was selected. This range could help to examine its effect between 0.5 g/L and 6.5 g/L. the selected ranges of adsorbent dose and contact time are comparable with the previous works using corncob derived magnetic biochar (Mohan, Kumar and Srivastava, 2014; Habibi, Rouhi and Ramavandi, 2018).

Table 3.1: Experimental range and levels of independent variables

Factors		**Range and Levels**	
	Code	Minimum (-1)	Maximum (+1)
Adsorbent Dose (g/L)	A	2	5
pH	B	4	8
Contact Time	C	30	70
Initial concentration (mg/L)	D	10	20

The total number of the experiment (N) was estimated using the following equation, which consisting 4 independent process variables 16 factorial points, 8 axial points, and 6 replicate at the central points.

$$N = 2^n + 2n + n_c \Rightarrow 2^4 + 2*4 + 6 = 30 \quad (3.12)$$

Statistical analysis of the model was carried out through the CCD of the Design expert computer software. The model was validated by conducting laboratory experiments at optimum conditions. Statistically, the optimum conditions were obtained by the following model equation:

$$Y = B_0 + \sum_{i=1}^{k} B_i X_i + \sum_{i=1}^{k} B_i X_i^{\,2} + \sum_{i>j}^{k} \sum_{j}^{k} B_{ij} X_i X_j + \varepsilon \quad (3.11)$$

Where; Y is a response of the process, i stands for linear coefficient and j represents quadratic coefficients, x_i and x_j are the independent variables, β_0 is standing for regression coefficient, k is the number of factors in the design, and ε represents an error.

3.12 Analyses on Groundwater Samples

After examining the initial pH and fluoride concentration in the collected groundwater samples, the batch adsorption test was conducted at optimum conditions predicted by RSM using the synthesized composite adsorbent.

3.13 Adsorbent Recyclability and Stability Test

In order to verify adsorbent reusability performance, the first fluoride ion from used LDMBC adsorbent was desorbed by washing 0.1 M NaOH solution for about 10 min. After dried the regenerated adsorbent, it was used again as an adsorbent at optimum process condition that was predicted by RSM. Additionally, to evaluate adsorbent stability, iron-leaching tests were conducted by determining the iron concentration in the treated water using a calorimeter instrument.

3.14 Ethical Consideration

Ethical considerations were taken into account for the study to be sound and ideal. Sample collection, processing, and analysis followed scientific methods and producers. Furthermore, all concerned bodies were informed prior to the study get started, finally, the result of laboratory analysis ethically recorded and interpreted based on scientific producers.

CHAPTER FOUR

4. RESULT AND DISCUSSION

4.1 Characterization of Materials

4.1.1 Proximate analysis result

The proximate analysis results of coffee husk as presented in Table 4.1, moisture content, ash content, and volatile mater were 9.52%, 11.4%, and 28.34% respectively. These shows about 49.26% of the contents tend to leave the sample and resulted 50.74 % of remaining fixed carbon. The proximate result of coffee husk in this study is comparable with previously defined by works of literature (Dume, Berecha and Tulu, 2015). According to (Cheng and Li, 2018), yield of biochar reduced and ash content increased as pyrolysis temperature increased. This might be due to the conversation of organic compounds and water molecules into syngas. Cheng and Li also suggest coffee husk pyrolysis at 450 ^{o}C was taken as an optimum condition to get high fixed carbon.

Table 4.1 Proximate analysis result

Physical Composition	Moisture content	Volatile matter	Ash content	Fixed carbon	Yield at 450 ^{o}C for 2 hrs (limited oxygen)	Yield at 450 ^{o}C for 3 hrs (oxygen free)
Result (%)	9.52	28.34	11.4	50.74	39.74	40.071

The yield obtained after coffee husks pyrolysis at temperatures ranges from 350 °C to 550 °C varies from 43.5% - 31.6% (Cheng and Li, 2018). The resulted biochar yield at 450 ^{o}C was laid between the suggested ranges in the literature. The yield in oxygen limited and oxygen free environments were 39.74 % and 40.071% respectively. The yield reduction at lower pyrolysis time might be due to the surface oxidation of the sample in an oxygen environment. Beside the yield reduction, ash content increases in an oxygen environment; this is not preferred in surface modification process of carbon material. This showed slow pyrolysis in oxygen free environment is a preferred condition for biochar production process.

4.1.2 Physiochemical property

As shown in Table 4.2, from the two materials of biochar and LDMBC higher surface area ($233m^2/g$) and higher bulk density were observed for LDMBC. This bulk density increment indicates that the successful replacement of light functional groups with metal oxide dopants.

Table 4.2: Physiochemical properties of adsorbent materials

Parameters	Biochar (BC)	Lanthanum doped magnetic Biochar (LDMBC)
Bulk density (g/Cm^3)	0.452	0.619
Surface area (m^2/g)	87.4	233
pH	10.6	6.7
pH_{PZC}	4.4	8.3

The pH of row biochar becomes highly basic due to the presence of a number of hydroxyl functional groups on its surface. While pH value of lanthanum doped magnetic biochar shows, pH reduction compared with row biochar. This can be attributed to the reduction of hydroxyl groups from the surface after modification. The pH_{PZC} and surface area of LDMBC also becomes higher than the row biochar as shown above in Table 4.2. In general, Biochar modification using iron and lanthanum nanoparticles can change the physiochemical property of biochar regarding with its surface structure and porosity. Hence, LDMBC adsorbent was preferred for removal of fluoride ion due to having a good quality foer anionic remooval.

4.1.3 Point of zero charge value

The results of the point of zero charges (PZC) of row biochar and lanthanum doped magnetic biochar were observed as 4.4 and 8.3 respectively. From the point of zero charge concepts, the surface of any material surface dominated by positive charge in a solution when the solution pH is lower than its PZC value. In contrast, surfaces of materials become negative when the pH of the solution is above PZC (Fooladvand and Ramavandi, 2015).

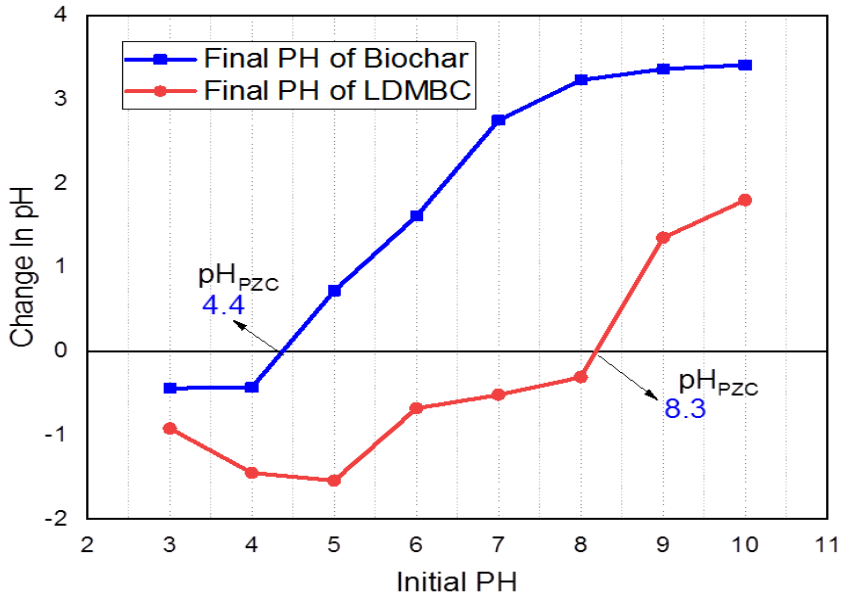

Figure 4.1 Point of zero charge value for biochar and lanthanum doped magnetic biochar

Since the point of zero charges of LDMBC is 8.3, it can be taken as energetic material to adsorb a negatively charged fluoride ion below the pH of the solution 8.3. While the row biochar PZC of 4.4 indicates that the material surface could be dominated with OH^- species above solution PH 4.4, and it can be suitable for cationic removal in solution pH > PZC. The point of zero charges of LDMBC shows comparatively higher from recent work (Habibi, Rouhi and Ramavandi, 2018) in the literature. The PZC of lanthanum-modified biochar was 6.6 as reported by (Habibi, Rouhi and Ramavandi, 2018), while in this study, lanthanum doped magnetic biochar resulted higher pH_{PZC} as shown in Figure 4.1. This might be due to the protonation effects of iron compound on the surface of biochar beside to lanthanum.

Therefore, it can be concluded that biochar modification using lanthanum and iron nanoparticles showed a significant effect to alter the surface charges of row biochar. The biochar surface becomes positive after modification.

4.1.4 Fourier transform infrared spectroscopy analysis result

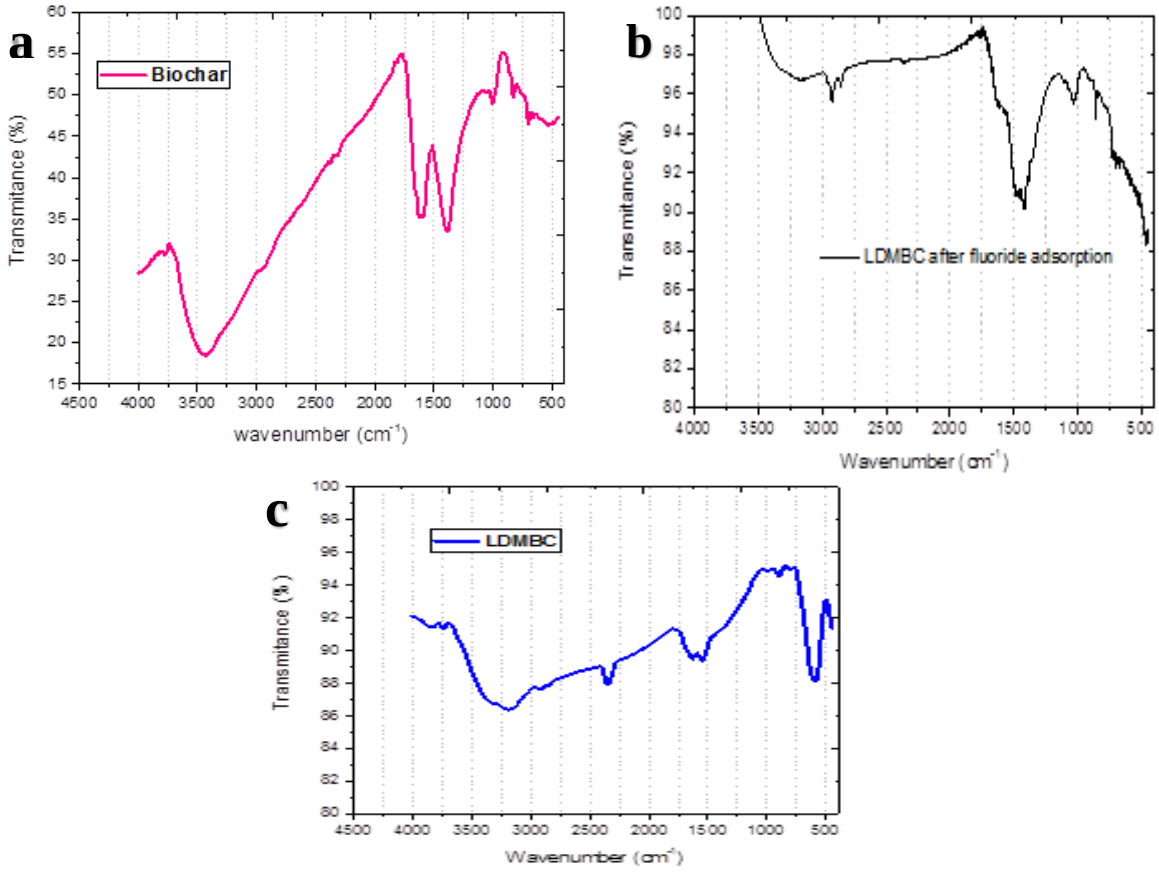

Figure 4.2: FTIR spectra analyses of materials

Biochar FTIR spectra analysis

As shown in Figure 4.2a, the FTIR spectra of coffee husk biochar display a number of sorption peaks, which indicate the presence of different functional groups. The biochar spectra graph displays a broad peak between 3680 and 2500 cm^{-1}. This represents the presence of free and bonded O–H functional groups. According to the infrared spectroscopy absorption table updated by (LibreTexts, 2019), the peaks observed at 1645 cm^{-1} may be assigned to strong C=O functional group. The peak at 1465cm^{-1} can be assigned to C-H and carboxylic acid. The other sharp peaks at 1000 and 695 cm^{-1} represent strong C-O and C=C respectively. The overall surface of biochar shows the presence of different negatively charged functional groups. Similar results have been reported continuously on different biomass-derived biochar including coffee husk biochar (Thanh and Tuan, 2016; Veiga Jenaina Ribeiro, 2017)

Table 4.3: FTIR spectra of biochar

Observed peak positions (cm^{-1})	Functional groups	Standard infrared spectroscopy absorbance region (LibreTexts, 2019)	Identity
3470	O-H	3700-3250 cm^{-1}	Strong, stretching
1645	C=O	1650 cm^{-1}	Strong, stretching
1465	C-H	1450-1330 cm^{-1}	Medium, bending
1010	C-O	1070-1050 cm^{-1}	Strong stretching
845	C=C	1050 -1150 cm^{-1}	Strong, bending

FTIR spectra of LDMBC before fluoride adsorption

As shown in Figure 4.2b, the lanthanum doped magnetic biochar clearly display that the reduction of hydroxyl, carboxyl, and carbonate functional groups after modification compared from row biochar. However, small peaks were observed at 3250, 2350, and 1625 cm^{-1}, which can be attributed to the existence of remaining O-H, C ≡N, and C-O groups. In addition, new peaks were observed at 560 and 625 cm^{-1}, which can be attributed to the presence of Fe–O and La–O bond respectively. The peaks assigned for these metal oxide compounds are in agreement with the previous related works reported by (Akbarnezhad and Safa, 2018) and (Wen, Wang, and Dong, 2015) correspondingly.

FTIR spectra of LDMBC after fluoride adsorption

Most of the peaks observed for the magnetic biochar nanocomposite material were weaker from the corresponding peaks of coffee husk biochar. Moreover, LDMBC adsorbent after treatment shows weaker peaks assigned for hydroxyl compared with adsorbent before the treatment process. Spectra of regenerated adsorbent display a new peak between 1400-1000 $cm^{-1,}$ which can reveal the existence of fluoro compounds as reported by (LibreTexts, 2019).

4.1.5 Thermogravimetric analysis

The thermal stability behavior of materials during pyrolysis is associated with the decomposition of cellulose, hemicellulose, and lignin or due to the releases of non-condensable syngas's, low molecular weight compounds like carboxylic aldehydes, alkenes, and other components. TGA curve of the biochar sample as shown in Figure 4.3, high mass losses were observed in four degradation zones. The mass loss at 100 ^{o}C was observed due to the releases of water molecules. High mass loss between 100 and 200 ^{o}C was observed; this may result in the degradations of low molecular weight compounds. High mass loss above 400 ^{o}C was also observed due to the decomposition of higher molecular weight compounds.

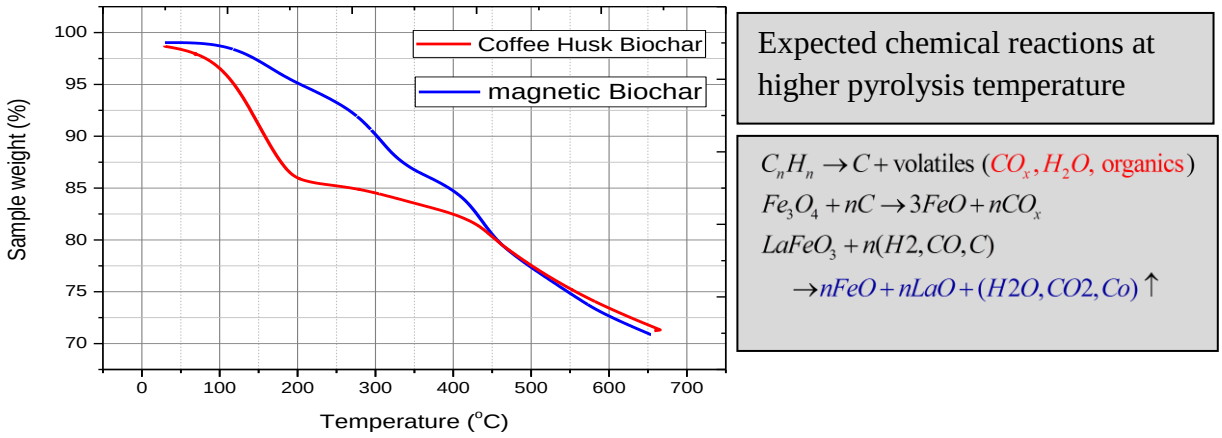

Figure 4.3 Thermogravimetric analyses of the adsorbent materials

The LDMBC curve as indicated in figure 4.3, high mass losses were observed above 450 ^{o}C. Decomposition at higher temperatures may be concerned with the reduction magnetite, hematite, and iron carbide composites into lower oxide groups as tried to describe in the above chemical reaction. This high decomposition of the magnetic composite at higher temperatures is expected due to the catalytic effects of iron species on the carbon surface (Sun *et al.*, 2019). Since the aim of synthesizing this magnetic biochar is for groundwater defluoridation application, the material stability in a hot stream of groundwater needs to be considered. The highest temperatures of hot stream water in the Rift Valley of Ethiopia were recorded being 112 ^{o}C in Dallol volcanic area (B. cavalazzi, R. Barbieri, F. Gomez, 2019). Therefore, the TGA analysis support that this composite material can be applied for water defluoridation in all volcanic and non-volcanic areas of Ethiopia.

4.1.6 X-ray diffraction analysis

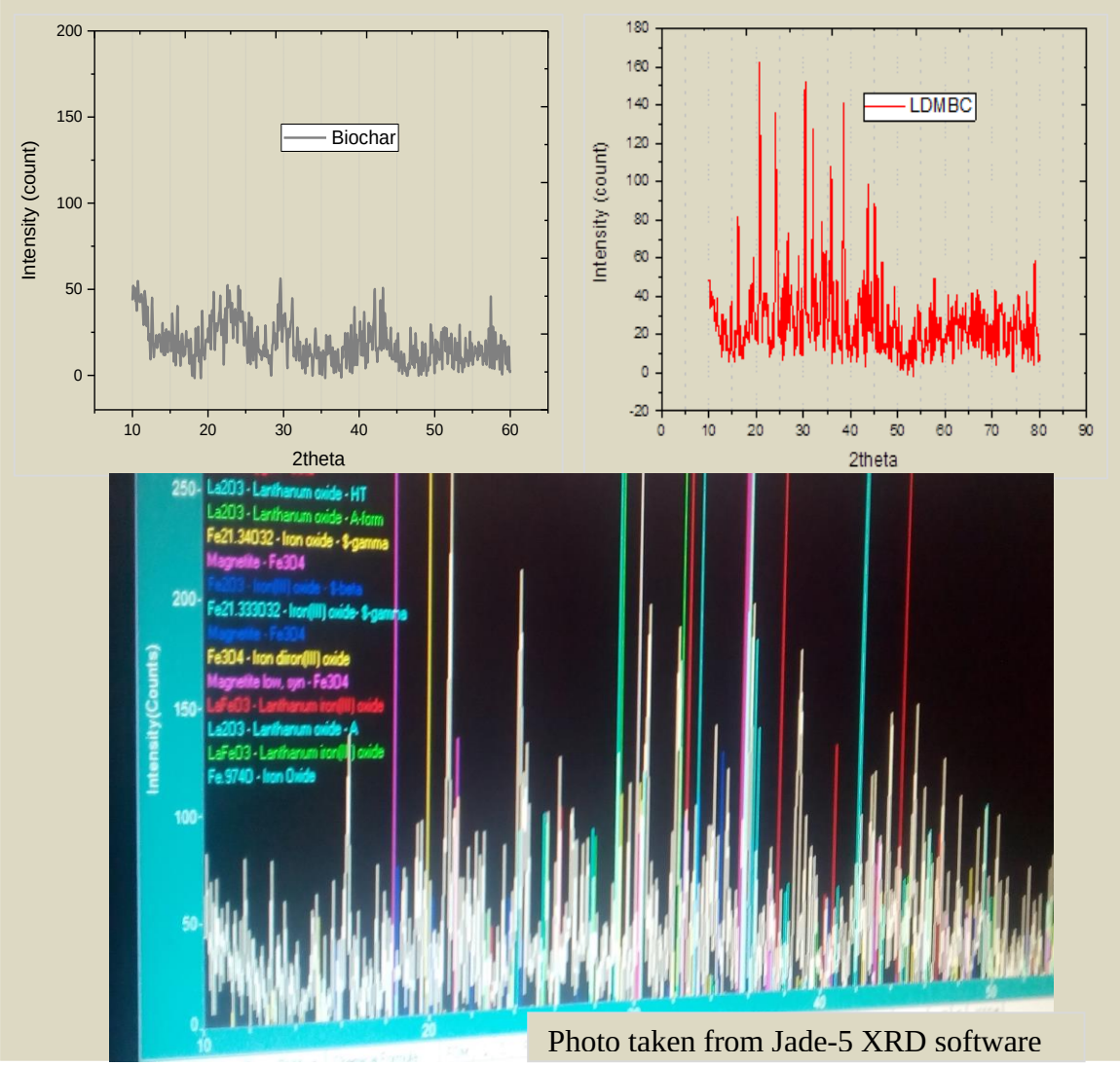

Figure 4.4 XRD analyses graphs of raw BC and LDMBC

The X-ray diffraction analysis (XRD) is used to measure the crystalline and non-crystalline phases of coffee husk biochar, and lanthanum doped magnetic biochar (LDMBC) composite materials. The crystalline structure of row biochar (Figure 4.4) is implying the non-crystalline amorphous structure. The XRD graph of LDMBC biochar after modification clearly shows the composite of magnetite (Fe_3O_4), hematite (Fe_2O_3), $LaFe_3O$ on the surface of amorphous background. These chemical compounds were clearly observed by analyzing XRD data using Jade-5 XRD software as shown in the photo.

The colors in the photo of software output clearly indicated peak positions of magnetite at 2theta of 30.4^{o}, 35.8^{o}, 38.5^{o}, 43^{o}, and 57.7^{o}. It is also clear that an extra sharp signal is observed at 24.12^{o} for composite formations of lanthanum with magnetic compounds. The peak positions of these iron compounds and lanthanum oxides have a similarity with previous works reported by (Akbarnezhad and Safa, 2018; Wen, Wang, and Dong, 2015).

Determination of average particle size

Average crystallite size of LDMBC adsorbent was determined from XRD data using the Scherrer's question. Initially as shown in Figure 4.5, the highest peak positions and FWHM were determined from XRD data using Originpro-2019 computer software, then the average crystalline size was determined using Microsoft excel by appling Scherrer's equation.

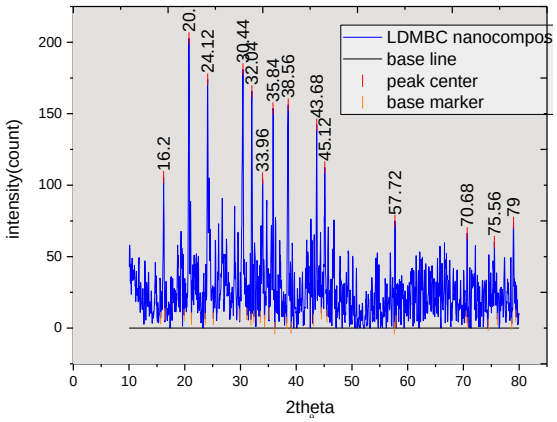

Figure 4.5 Peak center and FWHM calculation using origin software

The crystallite sizes of the selected highest peaks on modified biochar were varied from 32.41nm to 63.65 nm. The average particle sizes of metal oxide nanoparticles on the surface of amorphous background were 47.68 nm. Therefore, it can be concluded that the preparation of biochar-based nanocomposite adsorbent using lanthanum and iron salts through a chemical co-precipitation method was successfully achieved in Nano-scale.

4.1.7 Scanning electron microscopy analysis (SEM)

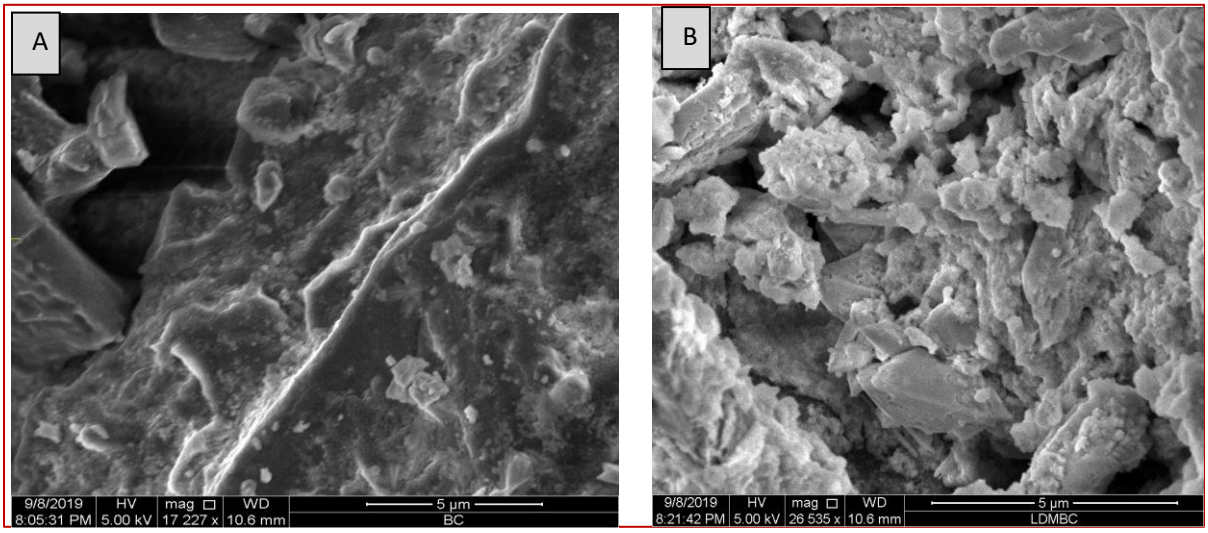

Figure 4.6 SEM images of BC and LDMBC

The above SEM images can clearly display the variation of biochar morphology before and after modification using metal oxide nanoparticles. The biochar SEM result is shown in Figure 4.6A display the heterogeneous layer with some high micromere structure. Whereas, LDMBC SEM image shown in Figure 4.6B displayed rough and white surface. In addition, numerous small pores were observed on lanthanum doped magnetic biochar compared with row biochar. This morphology change becomes with the activities of metal oxide nanoparticles on the surface of biochar. The appearance of pore on LDMBC adsorbent could be the reason for its surface area increment.

4.1.8 BET surface area analysis

BET surface area of BC and LDMBC were 87.4m^2/g and 233m^2/g respectively. The surface area increments in LDMBC may attribute to the activation properties of those metal salts $FeCl_3$ and $LaCl_3$ on biochar surface. The surface area increment after the magnetization process also reported in the previous works (Tu, 2017). The iron species can act as an activating agent to make micro and mesopore on the carbon surface (initially which have lower surface area); this leads to increase the surface area after modification (Cheng and Li, 2018). Conversely, some studies reported that the impregnation of metal nanoparticles on the surface of carbon material, which has initially high surface area, might block the pore area and resulting lower surface area after impregnation (Kakavandi *et al.*, 2013).

4.2 Data Analysis Using Response Surface Methodology (RSM)

4.2.1 Results of batch adsorption study

As previously mentioned, a CCD matrix was employed for conducting the experiments. The fluoride removal percentages measured according to the design matrix of the 30 runs and the corresponding predicted values obtained from the software were recorded in Table 4.4.

Table 4.4: Experimental run set up with actual and predicted values

Std.	Adsorbent Dose	pH	Contact Time	Initial Concentration	Final concentration	**Removal Efficiency**	
						Actual	Predicted
	g/L		Min	mg/L	mg/L	**%**	**%**
1	2	4	30	10	0.798	93.92	93.38
2	5	4	30	10	0.459	95.41	94.55
3	2	8	30	10	1.897	80.84	81.32
4	5	8	30	10	0.782	89.18	90.27
5	2	4	70	10	0.528	96.72	97.22
6	5	4	70	10	0.147	97.53	98.08
7	2	8	70	10	1.42	85.8	85.38
8	5	8	70	10	0.397	94.03	94.02
9	2	4	30	20	3.796	79.62	79.88
10	5	4	30	20	1.79	92.05	92.74
11	2	8	30	20	5.583	72.08	72.52
12	5	8	30	20	1.518	93.41	93.16
13	2	4	70	20	3.78	84.1	83.27
14	5	4	70	20	1.39	96.05	95.83
15	2	8	70	20	4.596	75.02	76.13
16	5	8	70	20	1.368	95.67	96.47
17	0.5	6	50	15	3.483	76.08	76.2
18	6.5	6	50	15	0.1875	98.75	97.71
19	3.5	2	50	15	1.6425	90.65	91.14
20	3.5	10	50	15	3.0495	80.73	79.73
21	3.5	6	10	15	2.379	87.74	87.71
22	3.5	6	90	15	1.074	95.34	94.86
23	3.5	6	50	5	0.0935	98.03	97.9
24	3.5	6	50	25	3.5425	87.23	86.85
25	3.5	6	50	15	0.891	95.36	93.86
26	3.5	6	50	15	0.7395	93.07	93.86
27	3.5	6	50	15	1.0485	95.01	93.86
28	3.5	6	50	15	1.053	92.28	93.86
29	3.5	6	50	15	1.1535	92.71	93.86
30	3.5	6	50	15	0.735	94.73	93.86

4.2.2 Development of regression model equation

Polynomial regression analyses resulted in a quadratic equation as the best response surface model for explaining the interaction between factors with the response variables in the defluoridation system. The quadratic model in terms of the coded factor along with the statistics is explained as follows

The model equation in terms of coded factors

$$\text{Efficiency}(\%) = +93.86 + 5.38A - 2.85B + 1.79C - 2.76D + 1.95AB + 2.92AD + 1.18BD - 0.1106CD - 1.73A^2 - 2.11B^2 - 0.6441C^2 \quad (4.1)$$

Where: - A: Adsorbent dose (g/L) B: pH C: Contact time (min) and D is Initial fluoride concentration (mg/L)

The positive sign in the regression modal indicates the positive effects of the factor for an increase in the response of the design. The negative sign indicates the decreasing effect of independent parameters on fluoride adsorption efficiency. The equation in terms of coded factors is important to determine the relative influence of process variables by comparing the coefficients of the variables.

Table 4.5: Fit statistics

Std. Dev.	1.05	R^2	0.9893
Mean	89.96	Adjusted R^2	0.9794
C.V. %	1.17	Predicted R^2	0.9628
		Model Precision	34.1407

The model showed a high significance level of 98.93% as refereed from $p < 0.0001$. The correlation coefficient (R^2) of the quadratic model showed its ability to explain over 95% of variances in the actual laboratory results. In addition, the adjusted correlation coefficient (R^2 adj) that adjusts R^2 value for the given number of relations was found to be very close to the correlation coefficient (R^2). This shows the high significance level of the suggested quadratic model. Furthermore, the values of standard deviation (SD) offered for the sound predictive ability of the generated quadratic model.

ANOVA results in Table A-6 indicate a Fisher's F-ratio of 92.53 that is greater than the critical P-value implying excellent fitting of the model to the experimental responses. Lack of fit test was also performed by the decomposing residual sum of squares into two components of lack of fit and pure error sum of squares.

The observed F-ratio of 0.3376 and the corresponding p-value of 0.9323 suggest the non-significance of lack of fit. This non-significance of lack of fit verifies model adequacy. Figure 4.7a demonstrates the plot of predicted versus experimental responses for fluoride removal by LDMBC. Grouping of the points around the sloping line indicates an acceptable fitting of the response surface model to the experimental fluoride removal efficiencies. The normal probability plot of the residuals was employed to distinguish the error in developing the quadratic model. Figure 4.7b demonstrates the satisfactory normal distribution of the residuals confirming that the residuals are independent of each other and that the error variances are homogeneous.

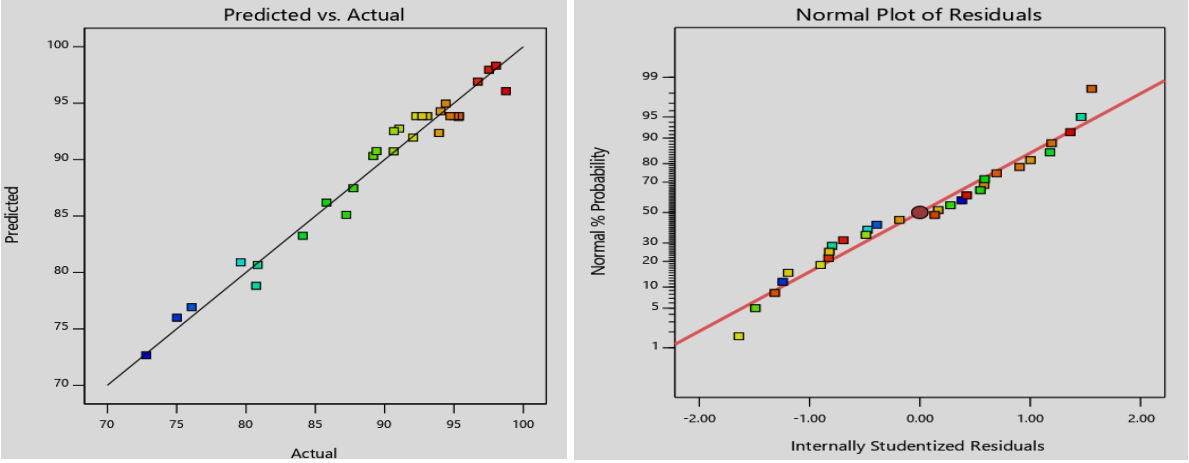

Figure 4.7: Graph of actual vs. predicted

Internal standardized residual is vital to check the goodness of data fit on the regression line under an established model. This implies that data was well fitted and is possible to predict the response under given ranges of process factors.

4.2.3 Effect of model parameters on fluoride removal efficiency

Based on the analysis of variance, the effects of each individual process variables and their interaction effects on the target response of percentage removal of fluoride were determined. RSM provided good information on the experimental data analysis in capturing individual process variables that significantly affect the defluoridation process.

According to ANOVA result in Table A-6, all first-order terms of A, B, C, and D and second-order terms of A^2, $B^{2,}$ and C^2 were highly significant to the response variable with a confidence of 98.93%. In addition, the two-factor interaction terms of AB, AD, and BD demonstrated significant effects on the fluoride removal efficiency at 95% confidence level. In the following graph, the perturbation curve shows the trends of all the factors effect with respect to the center point.

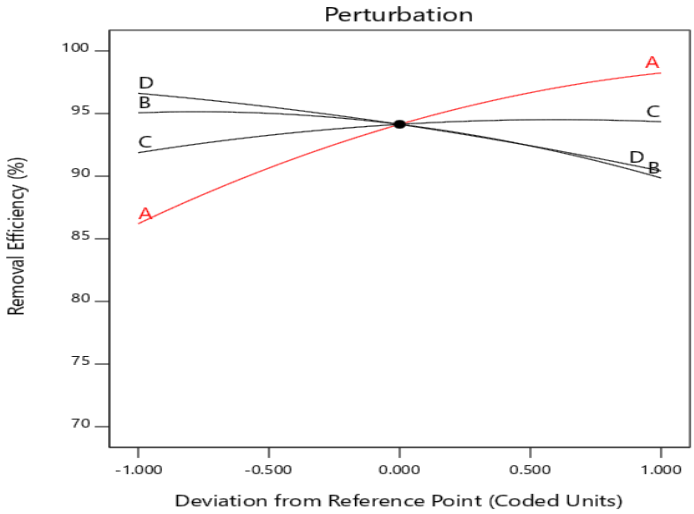

Figure 4.8: Perturbation curve of the dependant and independent variable

$$Percent\ of\ Contribution = \frac{SS}{\sum SS} * 100$$

Where: SS is values of sum of squares for all the model terms. The result shows the maximum contribution of 47.35 % for the adsorbent dosage followed by the second-order term of the variable with Percent of contribution value of 9.62%. Among the two-factor interaction effects, the highest level of contribution belonged to the interaction between the adsorbent dose and pH (PC = 3.12%). Total influences of first-order, second-order, and the two-factor interaction effects were valued as 75.736%, 16.82%, and 7.43% respectively.

4.2.3.1 Effect of adsorbent dosage

As shown in the 3D plot (Figure 4.9), the percentage of fluoride removal was significantly affected by adsorbent dosage. At a minimum dosage, limited surfaces provided for the adsorption process hence leading to lower removal efficiencies. However, as the dosage increase, more surfaces could be provided, and the removal becomes higher. The perturbation curve in Figure 4.8 also illustrating an increase in percentage removal with an increase in adsorbent dosage from 2-5 g/L. this indicates an increase in adsorption surfaces leads to increasing positive surface (Fe, La^{3+}, Fe^{3+}, $Fe^{2+,}$ etc.) of magnetic biochar nanocomposite adsorbent.

4.2.3.2 Effects of pH

The PH of the solution has a negative effect on the fluoride adsorption process (Figure 4.8). The result shows that as pH increasing from 2-6, the removal efficiency of fluoride increases slowly. Whereas, when the pH increases above pH 6, the removal efficiency decreased sharply. The decrease in the fluoride removal in basic solution is considered to be due to competition between fluoride and hydroxide ions. There are also similar results in the literature that can reveal the effect of pH on fluoride adsorption using lanthanum doped composite material (Habibi, Rouhi and Ramavandi, 2018).

4.2.3.3 Effects of initial concentration

The perturbation curve indicates that the increment of fluoride concentration would result in the decrement of the percentage removal of fluoride. The percentage removal of fluoride reduction due to an increase fluoride concentration could be attributed to; an increase in adsorbate concentration reduces adsorption sites, which were available on the magnetic biochar nanocomposite. When more ions were presented into the system at a certain time, then the system can become at a saturation phase. At minimum fluoride ions in the solution, more adsorption sites could be available and adsorption becomes higher compared to high fluoride concentration in the solution. Fluoride adsorption using the synthesized biochar based composite material showed that wide ranges of initial fluoride concentration can be removed using magnetic biochar nanocomposite adsorbent to meet WHO standards.

4.2.3.4 Effect of contact time

As shown in Figure (4.9), increasing contact time resulted in an increase in percentage removal of fluoride depicting that as time increases the fluoride ions were attached at the surface of the composite adsorbent more exhaustively.

4.2.4 Effect of interaction between process variables

The fluoride adsorption parameters were found to have high significance interaction effects on removal efficiency. The relatively higher interaction effect is observed between dose and concentration, dose and solution pH, and between pH and initial fluoride concentration.

4.2.4.1 Effect of variation in dosage and pH

As shown in Figure 4.9, when adsorbent dose increases, the percentage removal of fluoride also increased due to the availability of active sites for fluoride ion. As the adsorbent dose of the solution increased, the charge density of adsorbent surface increased until the pH increases from 2 to 6. This might result due to the affinities between fluoride ions and numerous species on the adsorbent surface. The result shows removal efficiency at pH 2 is lower and slightly increased when pH varies from 4-6. According to the previous work, fluoride in acidic solution can convert it into hydrogen fluoride, this might attribute to the reduction of efficiency in strongly acidic medium (Habibi, Rouhi and Ramavandi, 2018). In addition, reduction of removal efficiency at highly basic medium is related to the releases of OH^- in the solution. This negatively charged hydroxide ion can compete directly with fluoride ion.

4.2.4.2 Effects of variation in dosage with concentration

The response surface plot shown in Figure 4.9b depicted the interaction effects of initial concentration and adsorbent dose on percentage removal of fluoride. The removal efficiency increased with increasing adsorbent dosage and decreased with an initial concentration of fluoride. The maximum fluoride removal was achieved at the higher adsorbent dosage and lower fluoride concentration. This is because at this process conditions, a lower amount of fluoride concentration is sufficient to push the removal efficiency forward.

4.2.4.3 Effects of variation in pH with initial concentration

Interaction effects of initial concentration and solution pH shows a significant effect on fluoride removal efficiency as shown in the ANOVA Table A-6. When pH and concentration increases, the removal efficiency becomes decreased as shown in Figure 4.9c. This is because both pH and concentration affect the percentage of removal negatively. The maximum fluoride removal is achieved at the higher adsorbent dosage and medium pH of the solution.

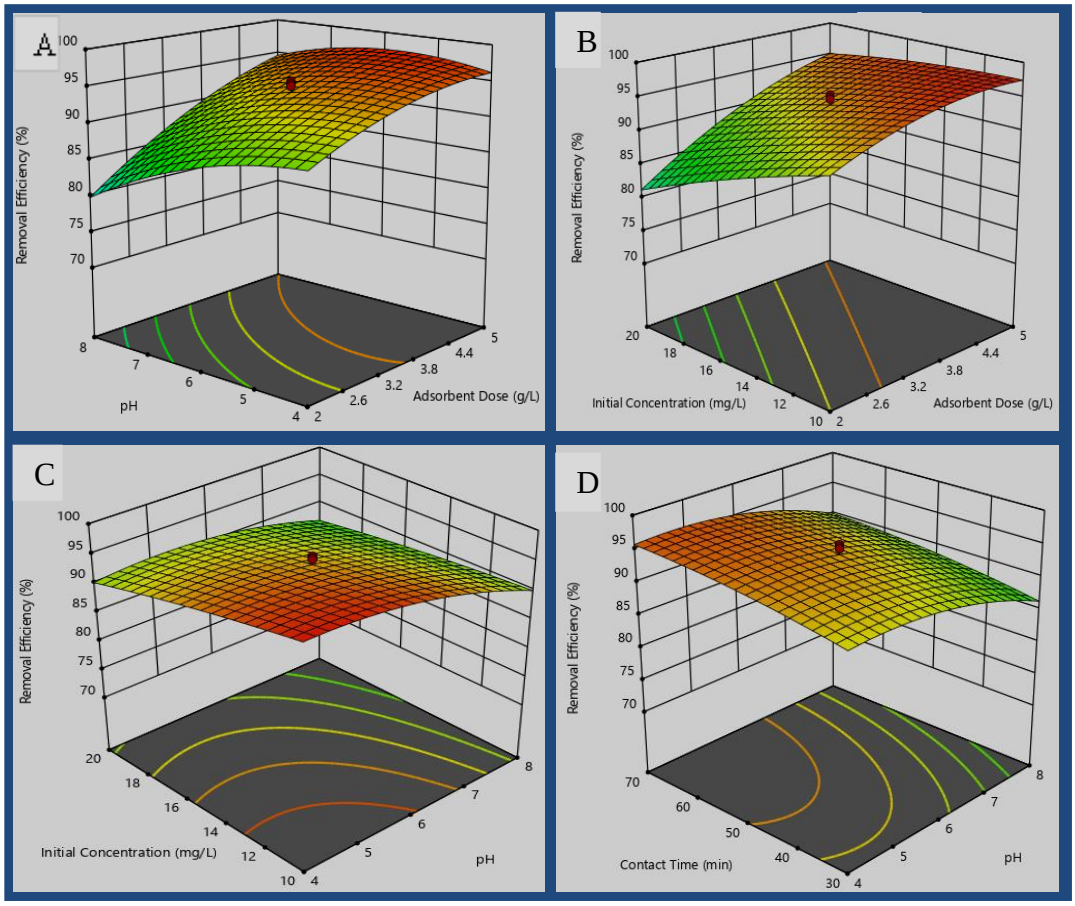

Figure 4.9: 3D plots of the major interaction effect of adsorption parameters

The above observations can easily be explained as higher adsorbent dosage and medium contact time will result in higher percentage removal, while medium Fluoride concentration will favor high contact time with increased adsorbent dosage. Moreover, higher contact time & medium fluoride concentration at medium adsorbent dosage will ensure the fluoride removal goes to the maximum value. The higher concentration, lower contact time, and the lower adsorbent dosage is not beneficial to maximizing the percentage removal of fluoride.

4.3 Optimization of Fluoride Adsorption process variables Using RSM

4.3.1 Numerical optimization

The targeted objective of the study is to maximize the fluoride removal efficiency using biochar based magnetic nanocomposite adsorbent. In the optimization process, different criteria were considered before obtaining the optimal conditions. By considering the interaction effects on the fluoride adsorption process, the constraints were developed as follows in table form.

Constraints

Table 4.6 constraint table for both defendant and independent parameters

Independent variables	Goal	Lower Limit	Upper Limit
A: Adsorbent Dose	is in range	2	5
B: pH	is in range	4	8
C: Contact Time	is in range	30	70
D: Initial Concentration	is in range	10	20
Removal Efficiency	Maximize	72.8	98.75

Fluoride adsorption efficiency was taken as a dependent variable in the optimization process.

Objective function

$$Y = f(A, B, C, \text{and } D) + \varepsilon \quad (4.2)$$

Where Y is the dependent variable (removal efficiency) and the independent variables; adsorbent dose, pH, contact time, and initial concentration were coded as A, B, C, and D respectively. Finally, the regression model equation was taken as an objective function.

$$\begin{aligned}\text{Removal Efficiency}(\%) = {} & +93.86 + 5.38A - 2.85B + 1.79C - 2.76D \\ & +1.95AB + 2.92AD + 1.18BD - 0.1106CD \\ & -1.73A^2 - 2.11B^2 - 0.6441C^2 - 0.3716D^2\end{aligned}$$

Finally, the software resulted in optimal conditions of fluoride adsorption process using lanthanum doped magnetic composite adsorbent within the given parameter ranges. The maximum fluoride removal of 98.994% was selected by the software from the hundred optional solutions.

Table 4.7: selected optimum solution predicted by RSM quadratic model

Number	Adsorbent Dose	pH	Contact Time	Initial Concentration	Removal Efficiency	Desirability	
1	**4.9184**	**5.754**	**59.993**	**12.245**	**98.994**	**1.000**	**Selected**

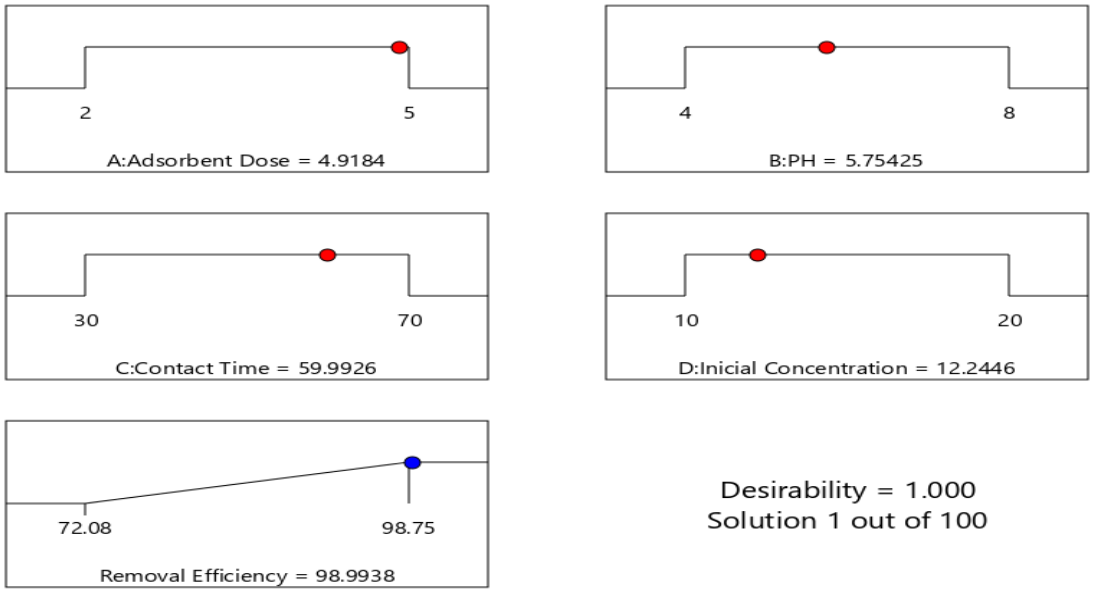

Figure 4.10: Optimum conditions in ramp style

To validate the model at optimum conditions, triplicate experiments were conducted using optimal process conditions of dose 5g, pH 5.754, contact time 60 min and initial concentration 12.245 mg/L. Considering maximum removal efficiency in the actual result, and both experimental and predicted values at the optimum point, the mean of the triplicates was 98.53%. Therefore, this study shows that coffee husk derived magnetic biochar nanocomposite adsorbent can definitely enhance fluoride removal from aqueous solutions.

4.4 Analysis of Fluoride Adsorption efficiency on Real Groundwater Samples

Defluoridation of the groundwater using LDMBC adsorbent at an optimum dose and contact time were conducted without adjusting the initial pH and Initial fluoride concentration. The final concentration and removal efficiency was presented in the following table. Based on the analysis results that were conducted at optimal process conditions using LDMBC adsorbent revealed that the material is efficient in the presence of other co-anions such as chloride nitrate, hydroxyl, and other anionic and cationic species.

Table 4.8 Physiochemical analysis on ground water samples before treatment

Sample area	pH	Chloride (mg/L)	Nitrate (mg/L)	Fluoride (mg/L)
Ziway	7.81	5.82	13.7	7.6
Meki	8.23	1.97	4.61	30.4
Alem Tena	7.67	21.03	1.113	11.4

Table 4.9 Analysis result on ground water samples after treatment using LDMBC adsorbent

Sample area	pH	Chloride (mg/L)	Nitrate (mg/L)	Fluoride (mg/L)	Efficiency (%)
Ziway	8.05	2.02	12.4	1.31	90.66
Meki	8.41	1.06	4.01	3.15	89.64
Alem Tena	7.85	17.53	0.4	1.01	91.14

The analysis conducted on the sample collected from Ziway caustic soda factory shows the reduction of fluoride concentration from 7.6 mg/L to 1.32 mg/L, which is within the allowable range of WHO guidelines. Although the analysis conducted on a sample collected from Meki town reduced the initial fluoride (30.4 mg/L) concentration to 3.15 mg/L, this result shows slightly higher than the standard limit (1.5 mg/L). This is due to the presence of interfering anions (Cl^-, NO_3^-, OH^- and other ions) and due to the increment of initial fluoride concentration above predicted optimum value (12.245 mg/L).

The removal efficiency on ground water samples has reduced compared with the synthetic solution at optimum condition. Compared with chloride and nitrate, high reduction of fluoride concentration was observed for all samples, these shows the adsorbent surface has high affinity with fluoride compared with the other onions in the solution. Therefore, the analysis revealed that Lanthanum doped magnetic biochar could be applicable in wide ranges of pH and fluoride concentration with the presence of co-anions in the solution.

4.5 Adsorbent Recyclability Test

In order to verify adsorbent reusability performance, the used magnetic biochar adsorbent was recycled five times at an optimum process condition that was predicted by the design expert. As shown in Figure 4.11 the three consecutive runs using magnetic biochar nanocomposite adsorbent was not demonstrated the high apparent reduction in the efficiencies of fluoride removal from water. However, it was observed that the efficiency decline from 98.51 to 89% after five consecutive cycles. This can be due to active cites leaching to the fluoride ion and blockage of the active sites by adsorbent materials.

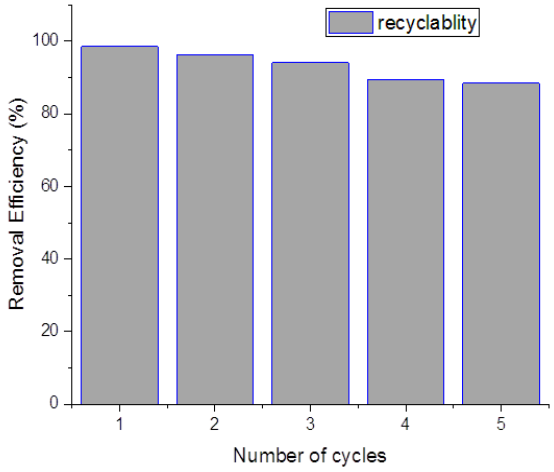

Figure 4.11: Reusability performance of LDMBC adsorbent

The result shows highest recyclability performance compared with the other adsorbents (Habibi, Rouhi and Ramavandi, 2018; Wen, Wang and Dong, 2015)

4.6 Stability of the Adsorbent

To examine the stability of LDMBC adsorbent in the application of fluoride treatment, an iron-leaching test was conducted at different pH values. The total mean iron concentration after treatment at pH 2, pH 6, and pH 10 were 0.13, 0.04, and 0.03 mg/L respectively. This shows that the iron concentration after treatment is less than that of the standard iron concentration (2 mg/L) in drinking water. According to (WHO report, 2018), the iron concentration in drinking water was described in three categories, maximum limit set (2 mg/L), medium set value (0.3), and the minimum level set of 0.2 mg/l. however, according to the study, iron concentration below 2 mg/L does not present a hazard to health. Therefore, it can be concluded that the synthesized biochar based magnetic nanocomposite adsorbent is stable in wide ranges of PH value.

4.7 Comparison of LDMBC with Other Fluoride Removal Adsorbents

Table 4.10: Comparison of LDMBC with Other Fluoride Removal Adsorbents

Adsorbent	Optimum Conditions	Efficiency (%)	Reference
LDMBC	Dose 6g/L, pH 5.764, time 60 min and concentration 12.245 mg/L	98.994	This study
Iron modified Biochar	At pH 6, Dose 10 g/L,	90	(Xuebin *et al.*, 2018)
Magnetic biochar	At pH 2, contact time 50 min, and dose 0.75 g/L	90	(Mohan, Kumar and Srivastava, 2014)
Graphene oxide	At pH 2, adsorbent dose 10 g/L	98.2	(Roy, 2017)
Activated alumina	Dose 8g/L, pH 8, contact time 60 min and initial concentration 5 mg/L	60	(Patra *et al.*, 2018)

Lanthanum doped magnetic biochar composite adsorbent resulted highest efficiency at lower contact time, lower dosage, medium pH, and higher concentration compared with another fluoride adsorbents.

CHAPTER FIVE

5. CONCLUSION AND RECOMMENDATION

5.1 Conclusions

In this study, lanthanum doped magnetic biochar nanocomposite adsorbent was prepared by modifying the surface of coffee husk biochar using iron and lanthanum oxide nanoparticles through chemical co-precipitation method and it was employed as an adsorbent for water defluoridation application. The FTIR analysis clearly proved that the fluoride removal by this adsorbent was the result of the surface ion exchange process. Based on the developed regression quadratic model, the adsorbent dosage with contribution of 47.3 % was found to be the most significant factor that affects the removal efficiency. Total influences of first-order, second-order, and the two-factor interaction effects were valued as 75.736%, 16.82%, and 7.43% respectively.

The findings of this study also designated that the optimum levels of the experimental variables were 5 g/L for the adsorbent dosage 5.754 for solution pH, 60 min for contact time and 12.245 mg/L for initial fluoride concentration with predicted fluoride removal efficiency of 98.994%. The mean triplicate experimental value at optimum conditions resulted a removal efficiency of 98.51%, which authenticated the prediction capability of the proposed response surface model.

High reduction of fluoride concentration was observed for all synthetic and groundwater samples, this shows the high affinity of the adsorbent surface with fluoride ion compared with the other onions in the solution. Therefore, the analysis shown that Lanthanum doped magnetic biochar could be applicable in wide ranges of pH and fluoride concentration with the presence of co-anions in the solution. In general, the research work validated that the synthesized magnetic biochar nanocomposite can be used as an efficient and stable adsorbent for removal of fluoride from water and the process can be successfully optimized by the response surface modeling method.

5.2 Recommendations

To explore the possibility of commercial application of lanthanum doped magnetic biochar nanocomposite material in the adsorption process of fluoride from water/wastewater; further investigations are recommended as follows.

1. Before the practical applications, further studies should be conducted on the physicochemical interfaces of this biochar-based magnetic nanocomposite material with the environmental media should be studied clearly.

2. In the synthesizing process, optimization studies on the surface area, porosity, and magnetic field strength of this biochar-based nanocomposite material should be studied clearly to enhance the adsorbent quality.

3. Furthermore, adsorption isotherm, kinetics, and thermodynamic parameters should be studied to examine the adsorption mechanism.

4. Column studies also recommended for evaluating the adsorbent and adsorbate relationship in the continuous adsorption configuration system.

Reference

Abd, A. M. E. and Rahman, E. (2014) 'Nanotechnology applications in water treatment : future avenues and challenges : A review', (June).

Akbarnezhad, A. A. and Safa, F. (2018) 'Biochar-based magnetic nanocomposite for dye removal from aqueous solutions : Response surface modeling and kinetic study 1', 91(11), pp. 1856–1866. doi: 10.1134/S1070427218110174.

B. cavalazzi, R. barbieri, F. Gomez, M. hago. (2019) 'The dallol geothermal area, northern afarnational planetary field analog on earth.pdf'.

Bekele Abaire, F. Z. & M. E. (2009) 'Operational experiences on small-scale community defluoridation systems'.

Bhattacharya, S. (2017) 'Application of nanostructured materials in fluoride removal from contaminated groundwater', pp. 87–93.

Boshir, M. *et al.* (2016) 'Progress in the preparation and application of modified biochar for improved contaminant removal from water and wastewater', *Bioresource Technology*. Elsevier Ltd, (May). doi: 10.1016/j.biortech.2016.05.057.

Dahi, E. (2016) 'Africa's u-turn in defluoridation policy: from the nalgonda technique to bone char', 49(December), pp. 401–416.

Domingues, R. R. *et al.* (2017) 'Properties of biochar derived from wood and high-nutrient biomasses with the aim of agronomic and environmental benefits', (May). doi: 10.1371/journal.pone.0176884.

Dume, B., Berecha, G. and Tulu, S. (2015) 'Characterization of biochar produced at different temperatures and its effect on acidic nitosol of jimma , southwest ethiopia', (July).

Fooladvand, M. and Ramavandi, B. (2015) 'Adsorption potential of NH4Br-soaked activated carbon for cyanide removal from wastewater', (September).

Gingasu, D. *et al.* (2011) 'Investigation of magnetite formation in the presence of hydrazine dihydrochloride', *digest journal of nanomaterials and biostructures*, 6(3), pp. 1065–1072.

Habibi, N., Rouhi, P. and Ramavandi, B. (2018) 'Modification of tamarix hispida biochar by

lanthanum chloride for enhanced fluoride adsorption from synthetic and real Wastewater', pp. 1–8. doi: 10.1002/ep.13026.

Hien, T. T. *et al.* (2017) 'Synthesis of novel magnetic adsorbents from', 55(4), pp. 526–533. doi: 10.15625/2525-2518/55/4/9016.

Jimenez, T. bolat; E. D. M. (2018) 'Modification of tea biochar with Mg, Fe, Mn and Al salts for efficient sorption of phosphate from aqueeous solutions'.

Kakavandi, B. *et al.* (2013) 'Synthesis and properties of Fe_3O_4 -activated carbon magnetic nanoparticles for removal of aniline from aqueous solution : equilibrium , kinetic and thermodynamic studies', pp. 2–10.

Kanyora, A. *et al.* (2015) 'Fluoride removal capacity of regenerated bone char in treatment of drinking water', (March).

Khichar, M. and Kumbhat, S. (2015) 'Defluoridation-A review of water from aluminium and alumina based compound', 2(5), pp. 4–11.

LibreTexts, C. (2019) 'Infrared spectra of some common functional groups'. available at: https://status.libretexts.org/.

Macdonald, A. and Dochartaigh, B. Ó. (2009) 'Mapping for Water Supply and Sanitation (WSS) in Ethiopia Research-inspired Policy Ethiopia and the Nile region Mapping for Water Supply and Sanitation (WSS) in Ethiopia', (January).

Malago, J., Makoba, E. and Muzuka, A. N. N. (2017) 'Fluoride Levels in Surface and Groundwater in Africa : A Review 2 . Sources of Fluoride in Surface and Groundwater in Africa', 3(1), pp. 1–17. doi: 10.11648/j.ajwse.20170301.11.

Melaku, Z. (2015) 'Perception on fluoride related health problems in an area of endemic fluorosis in Ethiopia : An exploratory qualitative study', (January 2002). doi: 10.4314/ejhd.v16i1.9830.

Mobeen, N. and Kumar, P. (2017) 'Defluoridation techniques - a critical review', 10(6).

Mohan, D., Kumar, S. and Srivastava, A. (2014) 'Fluoride removal from ground water using magnetic and nonmagnetic corn stover biochars', *Ecological Engineering*. Elsevier B.V., 73,

pp. 798–808. doi: 10.1016/j.ecoleng.2014.08.017.

Mtalo, F. *et al.* (2015) 'Development of affordable adsorbent systems for arsenic and fluoride removal in the drinking water sources in Tanzania Prosun Bhattacharya , Berit Balfors , Roger Project reference :

Nabizadeh, R. and Sadjadi, S. (2015) 'Modelling the effects of competing anions on fluoride removal by functionalized polyacrylonitrile coated with iron oxide nanoparticles', pp. 201–207.

Patra, G. *et al.* (2018) 'Removal of fluoride from wastewater using HCl-treated activated alumina in a ribbed hydrocyclone separator'. Taylor & Francis, (April). doi: 10.1080/10934529.2018.1429728.

Rajeswari, T. R., Kalpana, T. and Sailaja, N. (2016) 'International Journal of Modern Health Impacts of Fluorosis', 3(329), pp. 329–334.

Rechcigl, J. E. *et al.* (2015) 'Suitability of two methods for determination of point of zero charge (PZC) of Adsorbents in Soils', (November). doi: 10.1080/00103624.2015.1108434.

Rouzbahani, N. *et al.* (2017) 'Dental Fluorosis prevalence of children and drinking water fluoride level in bahar city of iran', 5(4), pp. 314–319. doi: 10.21276/sajb.

Roy, S. (2017) 'Synthesis of graphene oxide using tea-waste biochar as green substitute of graphite and its application in de-fluoridation of contaminated water'.

Salifu, A. (2017) Fluoride removal from groundwater by adsorption technology.

Samanta, Das, R. and Bhattachajee, C. (2016) 'Influence of nanoparticles for wastewater treatment- a short review', 3(3), pp. 1–6.

Sara Datturi, assefa kumsa, seifu kebede, f. van s. and m. van b. (2017) 'the right to smile: fluoride and fluorosis in central rift valley (ethiopia)', (january).

Science, W. and Chen, J. (2017) 'Magnetic biochar combining adsorption and separation recycle for removal of chromium in aqueous', (December 2016). doi: 10.2166/wst.2016.610.

Shah, M. S. and Foundation, D. (2016) 'Awareness about fluorosis – a survey', 8(6), pp.

530–532.

Sharma, M. *et al.* (2018) ‘Magnetic nanoparticles as an effective adsorbent for removal of fluoride – a review’, 3(3), pp. 207–210. doi: 10.15406/mojes.2018.03.00088.

Singh, J. (2016) ‘Fluoride ions vs removal technologies : A study’, *Arabian Journal of Chemistry*. King Saud University, 9(6), pp. 815–824. doi: 10.1016/j.arabjc.2014.06.005.

Soares, Veiga Jenaina Ribeiro, M. P. (2017) ‘Different plant biomass characterizations for biochar production’, (February 2018). doi: 10.1590/01047760201723042373.

Sun, Y. *et al.* (2019) ‘Multifunctional iron-biochar composites for the removal of potentially toxic elements , inherent cations , and hetero-chloride from hydraulic fracturing wastewater’, *Environment International*. Elsevier, 124(October 2018), pp. 521–532. doi: 10.1016/j.envint.2019.01.047.

Tan, X. *et al.* (2016) ‘Bioresource technology biochar-based nano-composites for the decontamination of wastewater : A review’, *Bioresource Technology*. Elsevier Ltd, 212, pp. 318–333. doi: 10.1016/j.biortech.2016.04.093.

Tang, Q. *et al.* (2019) ‘Science of the total environment preferable phosphate removal by nano-La (III) hydroxides modified mesoporous rice husk biochars : Role of the host pore structure and point of zero charge’, *Science of the Total Environment*. Elsevier B.V., 662, pp. 511–520. doi: 10.1016/j.scitotenv.2019.01.159.

Tekle-Haimanot and Mekonnen, Y. (2006) ‘Fluoride levels in water and endemic fluorosis in ethiopian rift valley’, pp. 12–16.

Thanh, N. D. and Tuan, P. D. (2016) ‘Optimizing the process of transforming coffee husks into biochar by means of hydrothermal carbonization’, 54, pp. 138–145.

Thermo scientific orion (no date) ‘manual delelectrodo de F-, Cat. N^{o} 9609 BNWP’.

Tu, Y. (2017) ‘Characterization and application of magnetic biochars from corn stalk by pyrolysis and hydrothermal treatment’, (July). doi: 10.15376/biores.12.1.1077-1089.

UKaid, natural environment research council, a. a. u. (2002) ‘improving access to safe drinking water: prospection for low fluoride sources’, (July), pp. 1–12.

Waghmare, S. S. and Arfin, T. (2015) ‘Fluoride removal from water by calcium materials : A State-Of-The-Art Review’, pp. 8090–8102. doi: 10.15680/IJIRSET.2015.0409013.

Wen, S., Wang, Y. and Dong, S. (2015b) ‘Performance and characteristics of fluoride adsorption using nanomagnetite graphite–La adsorbent’, *RSC Advances*. Royal Society of Chemistry, 5(October), pp. 89594–89602. doi: 10.1039/C5RA15215A.

WHO report (2018) ‘A global overview of national regulations and standards for drinking-water quality’.

Woldemarian, Daniel Ershad Khan, D. (2017) ‘New hope for hundred of millions suffering from poisoned well water’, pp. 1–22.

Xuebin, L. *et al.* (2018) ‘Simultaneous removal of fluoride and arsenic in geothermal water in Tibet using modified yak dung biochar as an adsorbent’.

APPENDIX A

Laboratory analysis result

Table A-1 proximate analysis result

Physical composition	W_1 (g)	W_2 (g)	Mass percentage (%)
Moisture content	6.5	5.8	MC=$\frac{w1-w2}{w1} * 100 = \frac{6.51-5.89}{6.51} * 100 = 9.52\%$
Volatile Matter	5.76	4.21	$VM = \frac{w1-w2}{w1} * 100 = \frac{5.75-4.12}{5.75} * 100$ =28.34%
Ash Content	6.4	0.73	AC= w_2/w_1= 0.73/6.4= 11.4 %
Fixed carbon	100-(%MC+%VC+%AC)= 100-49.26= 50.74 %		

Table A-2 Recorded data for zero point charge (PZC) examination

Sample number	The initial PH of row biochar and Lanthanum doped magnetic biochar	Final PH	
		Biochar	LDMBC
1	3	2.56	2.08
2	4	3.57	2.55
3	5	5.72	3.46
4	6	7.61	5.32
5	7	9.75	6.48
6	8	11.23	7.69
7	9	12.36	10.35
8	10	13.41	11.8

Table A-3 Calculated FWHM and Bragg angle data using origin

Peak no	FWHM(degree)	FWHM (radian)	2θ (degree)	θ (degree)	θ (radian)	D (nm)
1	0.17976	0.003137	16.2	8.1	0.1413717	44.79567
2	0.1951	0.003405	20.76	10.38	0.1811652	41.54164
3	0.19091	0.003332	24.12	12.06	0.2104867	42.70104
4	0.25364	0.004427	30.44	15.22	0.2656391	32.57342
5	0.1887	0.003293	32.04	16.02	0.2796017	43.95463
6	0.21917	0.003825	33.96	16.98	0.2963569	38.03215
7	0.15419	0.002691	35.84	17.92	0.312763	54.33949
8	0.25122	0.004385	38.56	19.28	0.3364995	33.61917
9	0.15972	0.002788	43.68	21.84	0.3811799	53.77265
10	0.21589	0.003768	45.12	22.56	0.3937463	39.98669
11	0.14345	0.002504	57.72	28.86	0.503702	63.45536
12	0.1526	0.002663	70.68	35.34	0.6167994	64.04298
13	0.16477	0.002876	75.56	37.78	0.6593854	61.21624
14	0.1932	0.003372	79	39.5	0.6894051	53.47631

For example, the crystallite size of the first highest peak at $2\theta = 16.2^{o}$ is calculated using Scherrer's equation as follows;

Scherrer's equation $D = \frac{k\lambda}{\beta \cos\theta}$

Where:- D=crystallite size (nm)

k=0.9 (Scherrer's constant)

λ=0.15406 (wavelength of the x-ray sources)

β=Full Width at Half Maximum (FWHM)

θ=peak position (radians)

$$D = \frac{0.9 * 0.15406nm}{0.003137*\cos(0.141372)} = 44.796 \text{ nm}$$

Table A-4 Batch adsorption result in terms of efficiency and capacity

Std.	Adsorbent Dose	PH	Contact Time	Initial Concentration	Final concentration	**Removal Efficiency**	
						Efficiency	Capacity
	g/L		min	mg/L	mg/L	%	mg/g
1	2	4	30	10	0.798	93.92	1.8404
2	5	4	30	10	0.459	95.41	1.9082
3	2	8	30	10	1.897	80.84	1.6206
4	5	8	30	10	0.782	89.18	1.8436
5	2	4	70	10	0.528	96.72	1.8944
6	5	4	70	10	0.147	97.53	1.9706
7	2	8	70	10	1.42	85.8	1.716
8	5	8	70	10	0.397	94.03	1.9206
9	2	4	30	20	3.796	79.62	3.2408
10	5	4	30	20	1.79	92.05	3.642
11	2	8	30	20	5.584	72.8	2.8832
12	5	8	30	20	1.518	93.41	3.6964
13	2	4	70	20	3.78	84.1	3.244
14	5	4	70	20	1.39	96.05	3.722
15	2	8	70	20	4.596	75.02	3.0808
16	5	8	70	20	1.368	95.67	3.7264
17	0.5	6	50	15	3.483	76.08	2.3034
18	6.5	6	50	15	0.1875	98.35	2.9625
19	3.5	2	50	15	1.6425	90.65	2.6715
20	3.5	10	50	15	3.0495	80.73	2.3901
21	3.5	6	10	15	2.379	87.74	2.5242
22	3.5	6	90	15	1.074	95.34	2.7852
23	3.5	6	50	5	0.0935	98.03	0.9813
24	3.5	6	50	25	3.5425	87.23	4.2915
25	3.5	6	50	15	0.891	95.36	2.8218
26	3.5	6	50	15	0.7395	93.07	2.8521
27	3.5	6	50	15	1.0485	95.01	2.7903
28	3.5	6	50	15	1.053	92.28	2.7894
29	3.5	6	50	15	1.1535	92.71	2.7693
30	3.5	6	50	15	0.735	94.73	2.853

Table A-5 BET surface area result

Horiba Instruments, Inc.
SA-9600 Series Surface Area Analyzer

Analysis Report
Sep/02/2019

Customer	: MERID D.	Operator ID	: SARA
Description	: Biochar based magnetic composite ad/t	Analysis Date	: Sep/02/2019
Filename	: BCBCA_6.sa2	Analysis Time	: 11:46:12

Condition Settings

Room Temp	: 24.0 (°C)	Atm. Pres	: 700.0 (mm)
Gas Used	: Nitrogen	Gas Conc	: 0.500, 0.250, 0.199 %

	Channel: 1	Channel: 2	Channel: 3
Sample Name	LANTHANUIM DOPED ME	MAGNETIC BIOCHAR	BIOCHAR
Tube Number	1	2	3
Tare Weight	10.1150 (gm)	10.1320 (gm)	10.0170 (gm)
Sample Weight	10.1520 (gm)	10.1500 (gm)	10.0550 (gm)
Degas Temp.	230 (°C)	230 (°C)	230 (°C)
Degas Time	60 (min)	60 (min)	60 (min)
Surface Area (M²/gm)	233.658	213.452	87.724
Slope	413.620	911.360	989.185
Intercept	-11.098	-5.594	54.759
Vm	0.002	0.001	0.001
BET Const	-36.269	-161.904	19.064
Pearson Coef	0.998	1.000	1.000
X[1] - 0.449	175.677	404.625	498.799
X[2] - 0.269	96.732	235.944	320.553
X[3] - 0.179	65.494	160.535	232.655

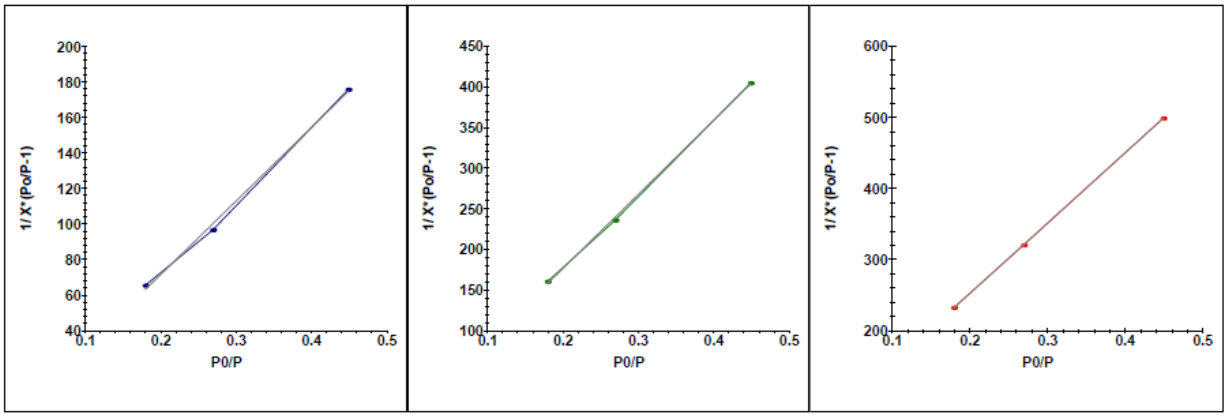

Table A-6 ANOVA result for Quadratic model

Source	Sum of Squares	df	Mean Square	F-value	p-value	
Model	1495.63	14	106.83	92.53	< 0.0001	Significant
A-Adsorbent Dose	734.16	1	734.16	635.91	< 0.0001	
B-PH	126.59	1	126.59	109.65	< 0.0001	
C-Contact Time	71.35	1	71.35	61.80	0.0001	
D-Initial Concentration	242.06	1	242.06	209.67	< 0.0001	
AB	48.44	1	48.44	41.96	< 0.0001	
AC	1.29	1	1.29	1.12	0.3075	
AD	44.42	1	44.42	38.48	< 0.0001	
BC	1.95	1	1.95	1.69	0.2138	
BD	13.51	1	13.51	11.70	0.0038	
CD	6.10	1	6.10	5.28	0.0363	
A^2	60.10	1	60.10	52.05	< 0.0001	
B^2	149.09	1	149.09	129.14	< 0.0001	
C^2	46.28	1	46.28	40.09	0.0001	
D^2	4.99	1	4.99	4.32	0.0552	
Residual	17.32	15	1.15			
Lack of Fit	6.98	10	0.6979	0.3376	0.9323	not significant
Pure Error	10.34	5	2.07			
Cor Total	1512.94	29				

Appendix B

Photos taken during laboratory works

Figure B-1: Sample Collection

Figure B-2: Visited fluoride treatment plants in ECRV areas

Figure B-3: Coffee husk Pyrolysis in the absence of oxygen

Figure B-4: Photo taken during adsorbent preparation

Batch adsorption experiment

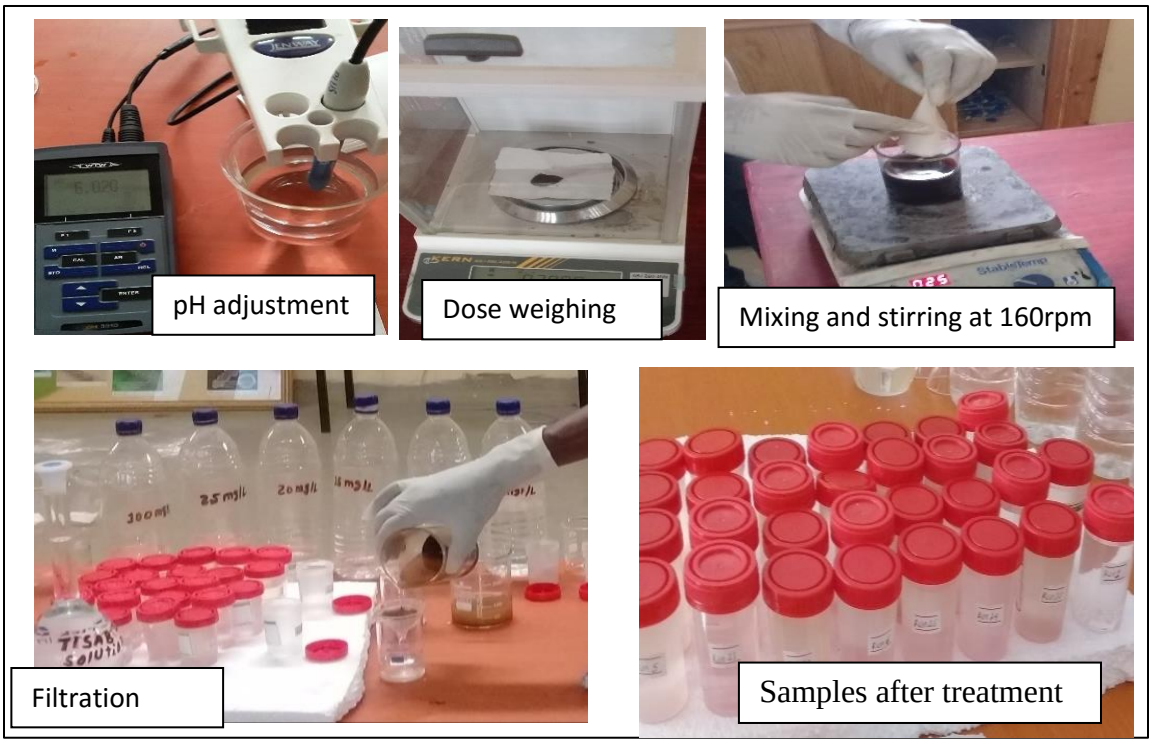

Figure B-5: Photos taken during adsorption process

Figure B-6: Photo taken during sample treatment for BET surface area analysis